Higgs Boson Production and Properties at ATLAS

Decays into Boson Pairs, and overall combination

EPS-HEP, Marseille, 9th of July 2025

Zef Wolffs on behalf of the ATLAS collaboration
University of Amsterdam and Nikhef institute

The Higgs boson's (short) history

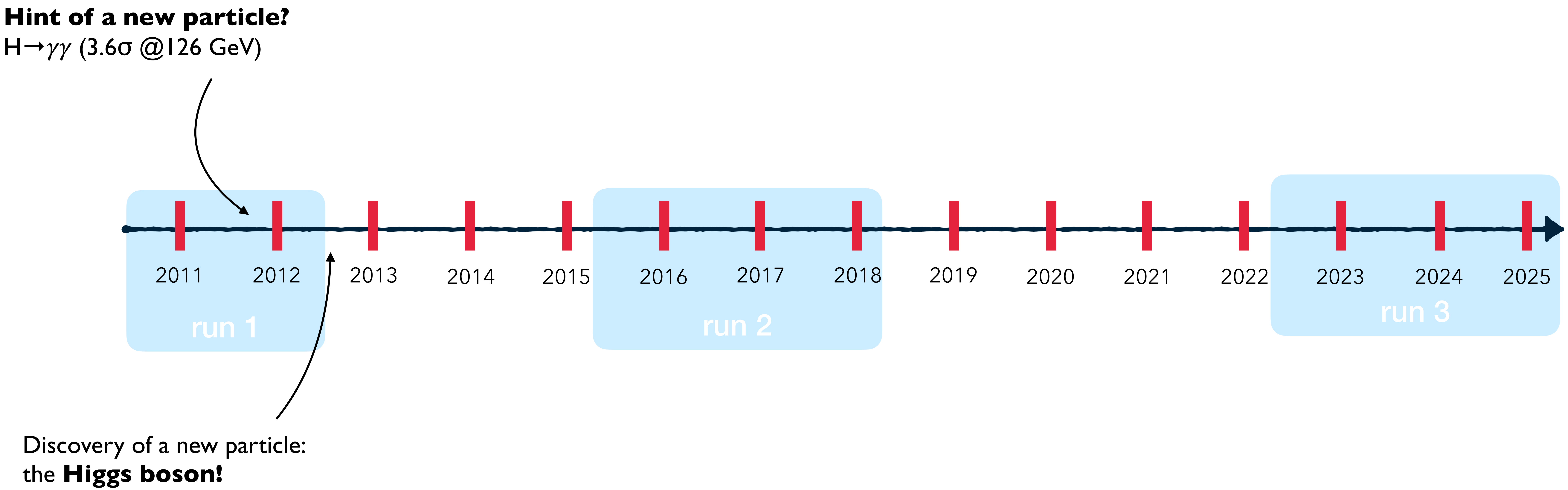

The Higgs boson's (short) history

Hint of a new particle?
H→$\gamma\gamma$ (3.6σ @126 GeV)

Shedding light on the **Spin nature** of the Higgs

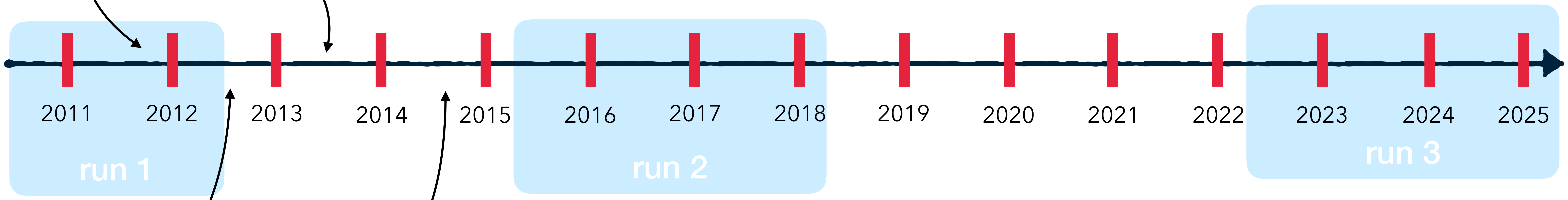

Discovery of a new particle: the **Higgs boson!**

First measurement of the **Higgs boson mass**

The Higgs boson's (short) history

Hint of a new particle?
H→$\gamma\gamma$ (3.6σ @126 GeV)

Shedding light on the **Spin nature** of the Higgs

A detailed map of Higgs interaction


Article
A detailed map of Higgs boson interactions by the ATLAS experiment ten years after the discovery


Article
A portrait of the Higgs boson by the CMS experiment ten years after the discovery

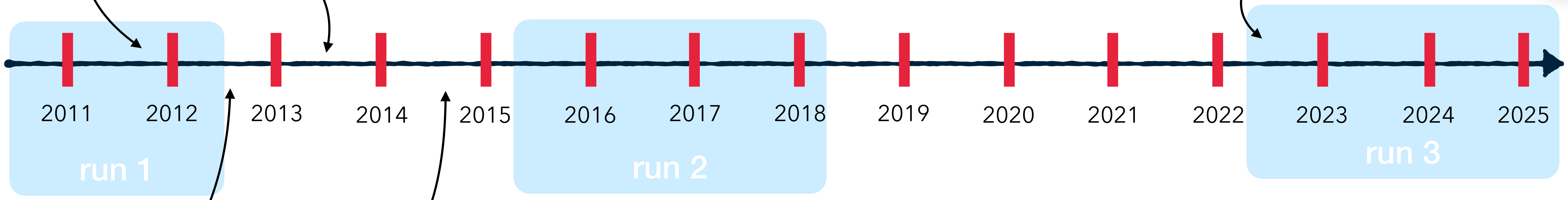

Discovery of a new particle: the **Higgs boson!**

First measurement of the **Higgs boson mass**

The Higgs boson's (short) history

Hint of a new particle?
H→$\gamma\gamma$ (3.6σ @126 GeV)

Shedding light on the **Spin nature** of the Higgs

A detailed map of Higgs interaction

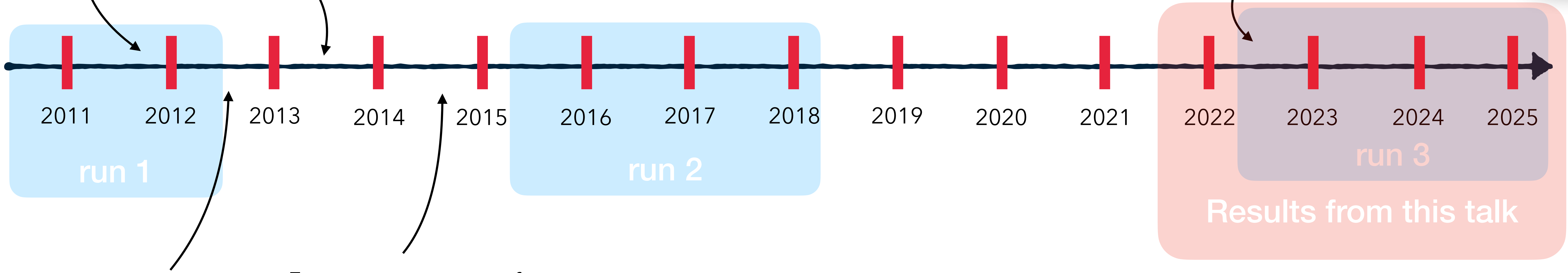

Discovery of a new particle: the **Higgs boson!**

First measurement of the **Higgs boson mass**

In just over a decade of Higgs physics we managed to clear the picture of the Higgs Boson, establishing its: mass, width, CP state, couplings, etc...

This talk focuses on:

- **Global combinations**
- **H->WW decays**
- **H->ZZ decays (in run 3!)**

The conclusion after a decade of Higgs physics?

Nature 607, 52–59 (2022)

To answer this question we can turn to the Higgs combination paper published in Nature

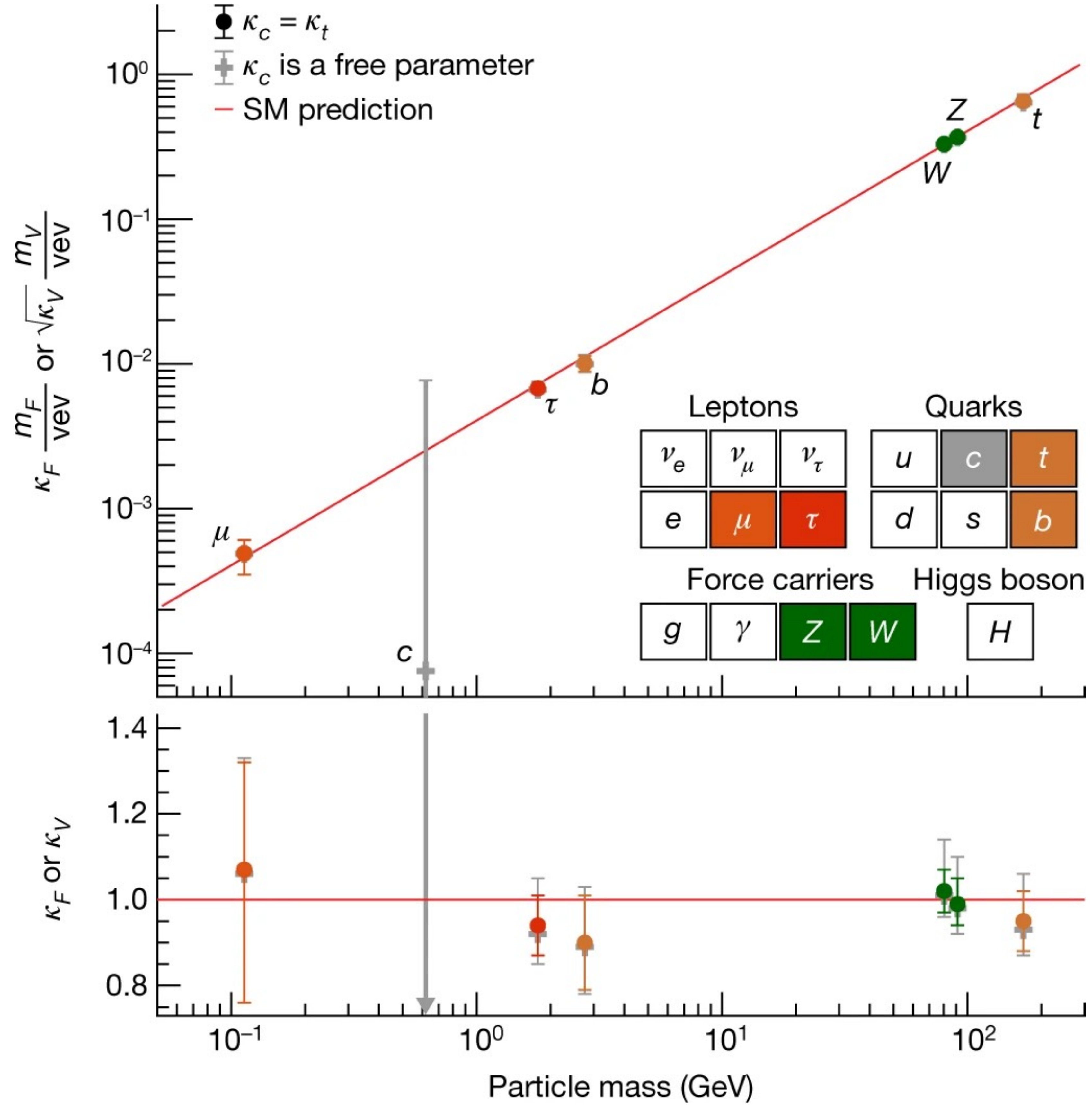

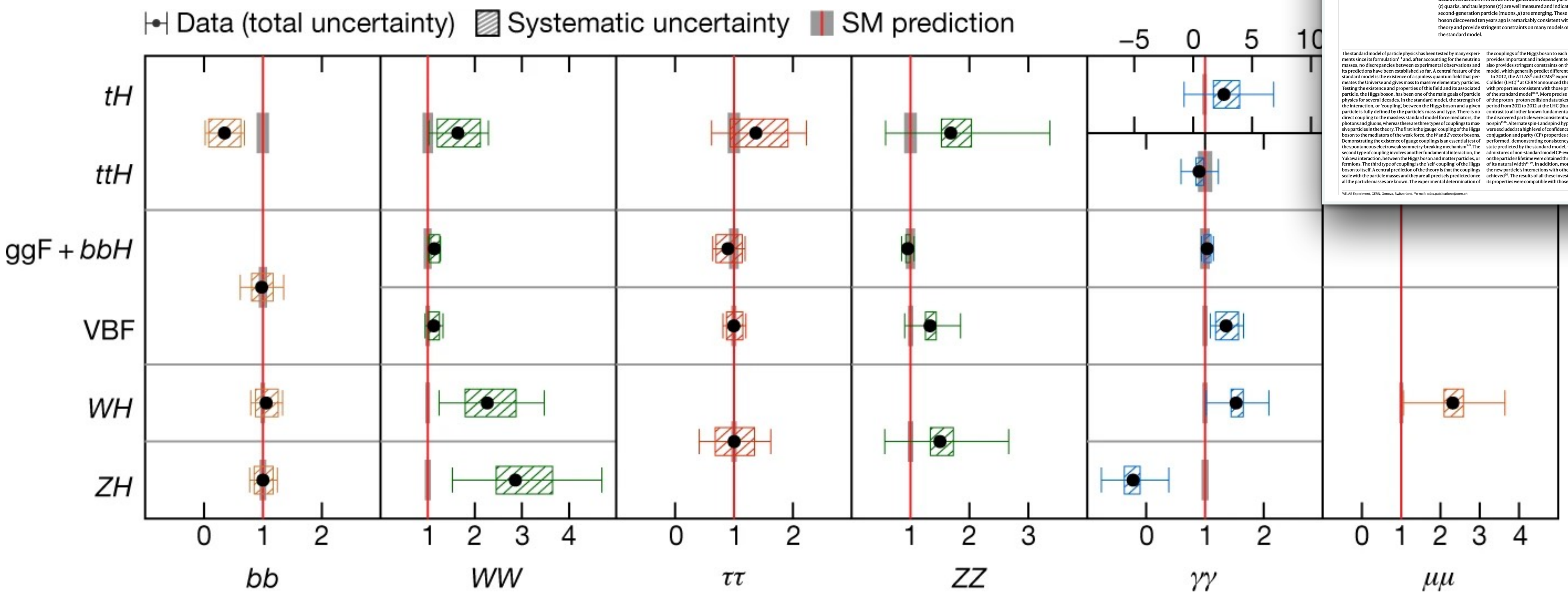

Interpretation in kappa framework

$$\sigma_i \times B_i = \frac{\sigma_i(\kappa) \times \Gamma_f(\kappa)}{\Gamma_H} \qquad \kappa_i^2 = \frac{\sigma_i}{\sigma_i^{SM}} \qquad \kappa_i^2 = \frac{\Gamma_i}{\Gamma_i^{SM}}$$

Answer: The Higgs mechanism in the standard model describes LHC physics excellently!

A new Higgs Boson combination analysis

CONF-2025-006
New for EPS-HEP!

Since the recent Higgs ("nature") combination paper **new results were made or improved**
→ these were combined into a new global combination

Analysis	Prod. modes	$\mathcal{L}$ (fb^{-1})	Reference	STXS stage	Improvements relative to Ref. [5]
$H \to \gamma\gamma$	All	140	[13]	1.2	-
$H \to ZZ^* \to 4\ell$	All	140	[14]	1.2	-
$H \to \tau\tau$	All	140	[15]	1.2	Reanalysis
$H \to WW^* \to \ell\nu\ell\nu$	ggF,VBF	140	[16]	1.2	Reanalysis
$H \to WW^* \to \ell\nu\ell\nu$	VH	140	[17]	1.2	Full Run 2
$H \to bb$	VBF	126	[7]	1.2	-
$H \to bb, cc$	VH	140	[18]	1.2	Reanalysis
$H \to$ multileptons	ttH	36.1	[6]	1.2	-
$H \to bb$	ttH	140	[19]	1.2	Reanalysis
$H \to \tau\tau$	VH	140	[20]	0	New analysis
$H \to Z\gamma$	All	140	[21]	0	-
$H \to \mu\mu$	All	140	[22]	0	-

The Higgs combination paper published in Nature

All the above analyses are combined for a measurement of the:
Inclusive cross section of Higgs production, cross sections per prod/decay mode, and coupling modifiers (κ framework)

A new Higgs Boson combination analysis

CONF-2025-006
New for EPS-HEP!

Results: high precision measurements of the Higgs boson!

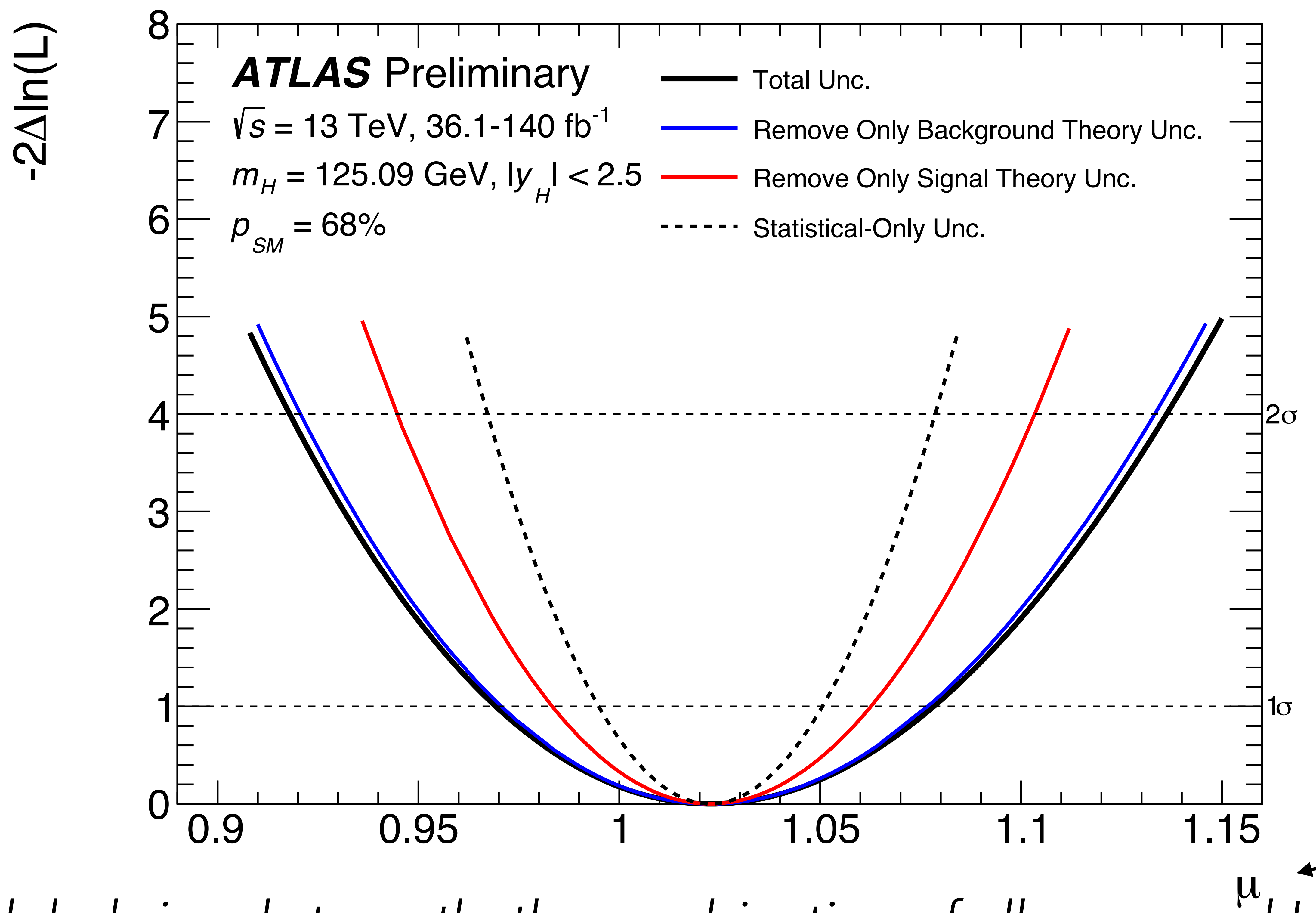

Global signal strength, the combination of all measured Higgs production and decay modes
- largest uncertainty: theoretical modelling of signal

$\mu_{if} = (\sigma_i \times B_f)/(\sigma_i^{\mathrm{SM}} \times B_f^{\mathrm{SM}})$

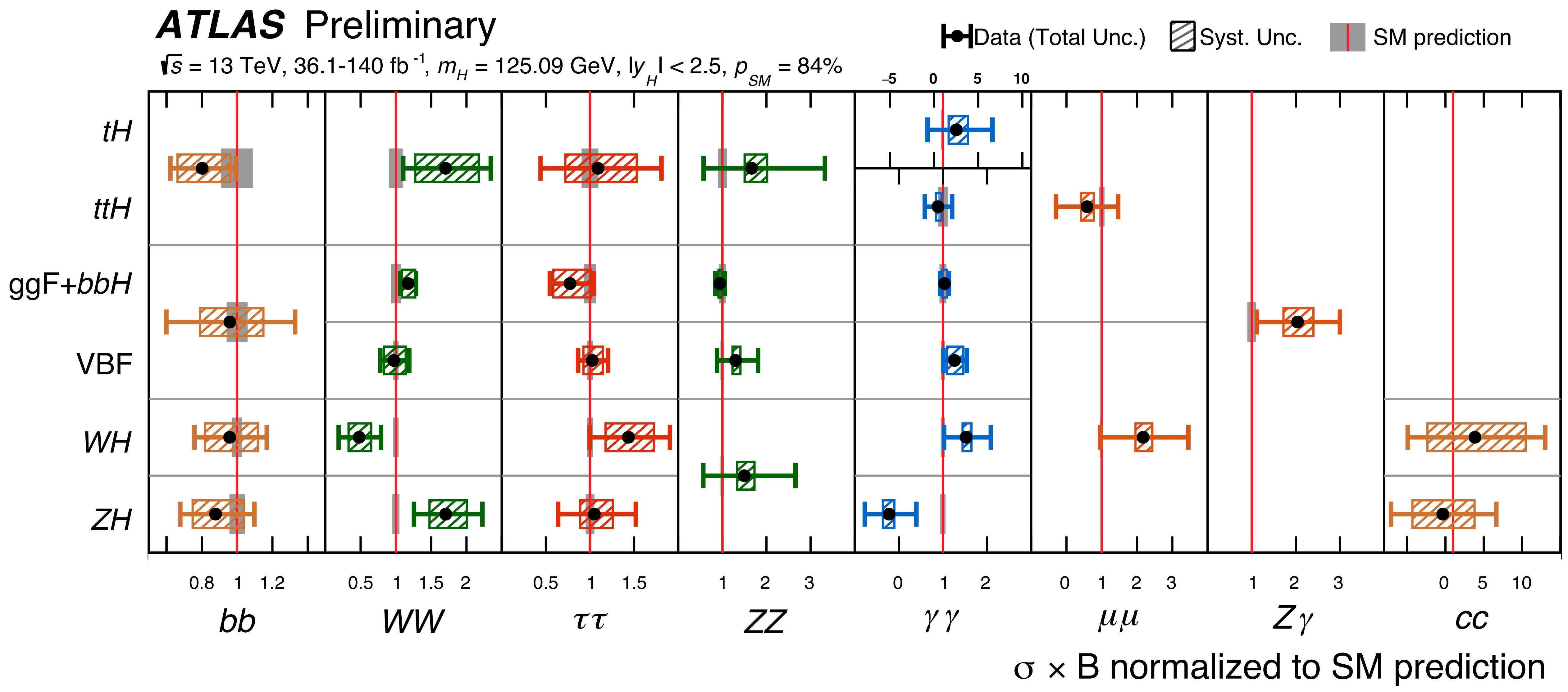

Cross-section times branching ratio ($\sigma \times$ B) by Higgs production and decay modes

A new Higgs Boson combination analysis

CONF-2025-006
New for EPS-HEP!

Testing the Yukawa mechanism with improved precision

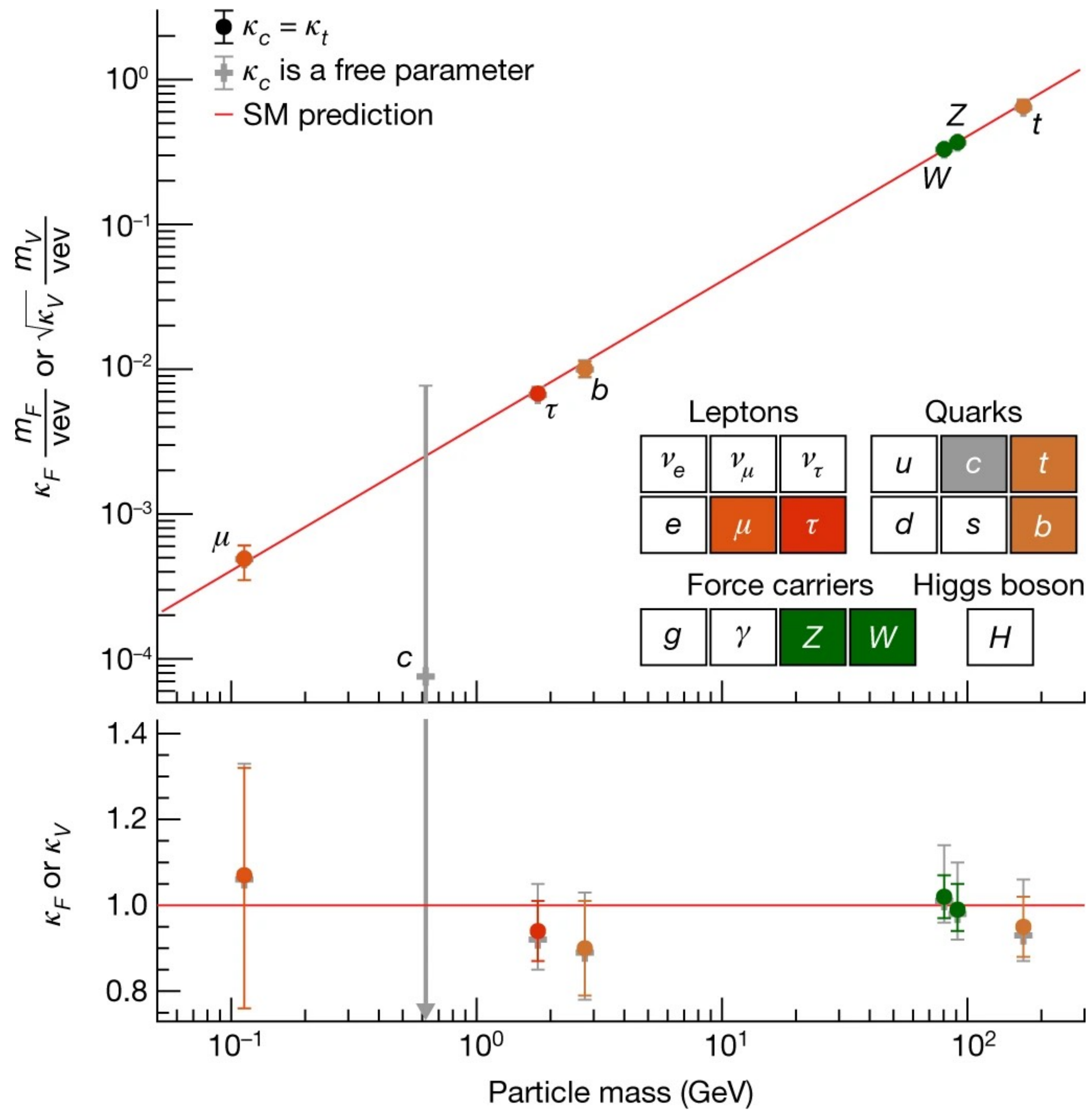

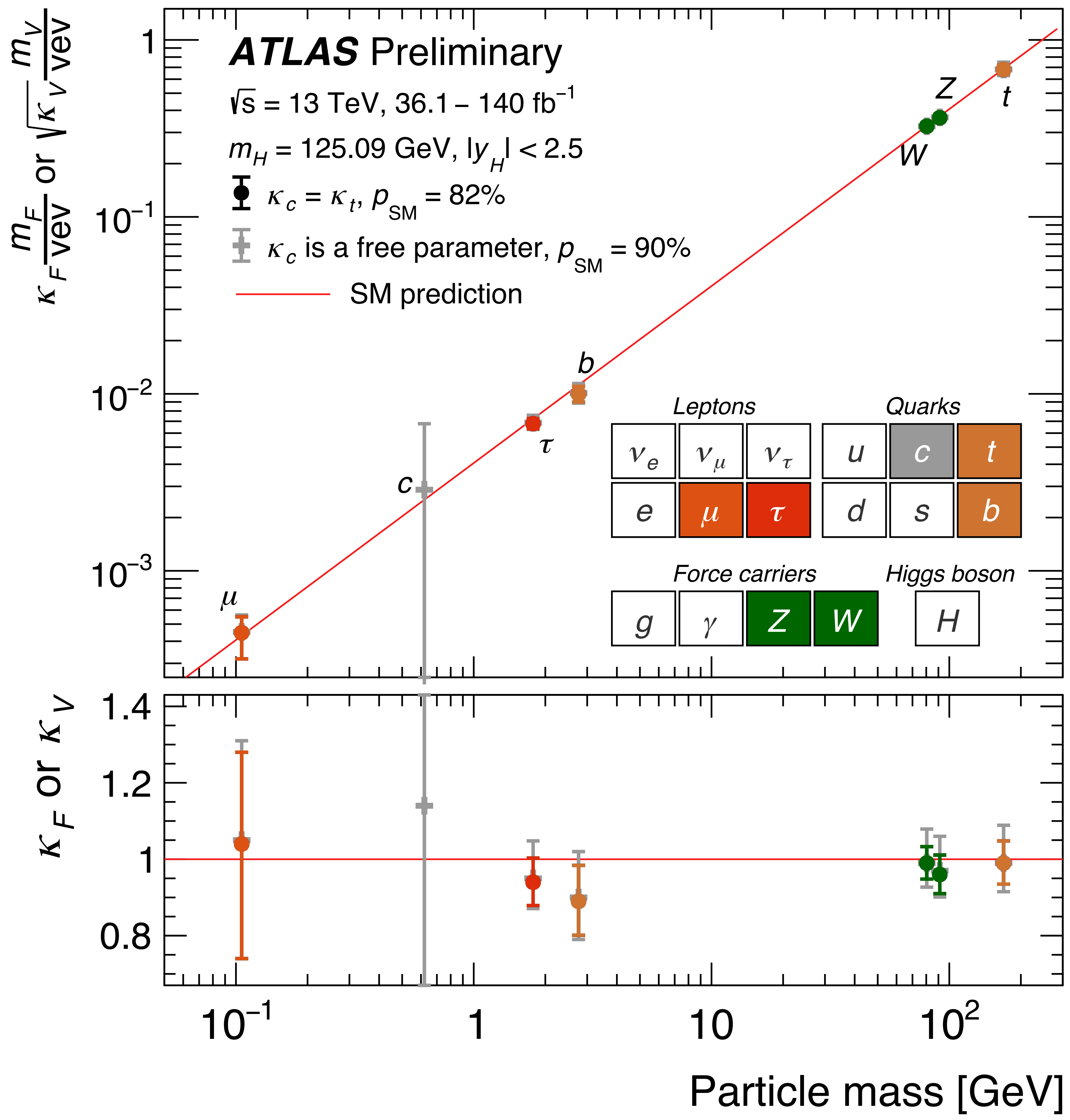

A new Higgs Boson combination analysis

CONF-2025-006
New for EPS-HEP!

Testing the Yukawa mechanism with improved precision

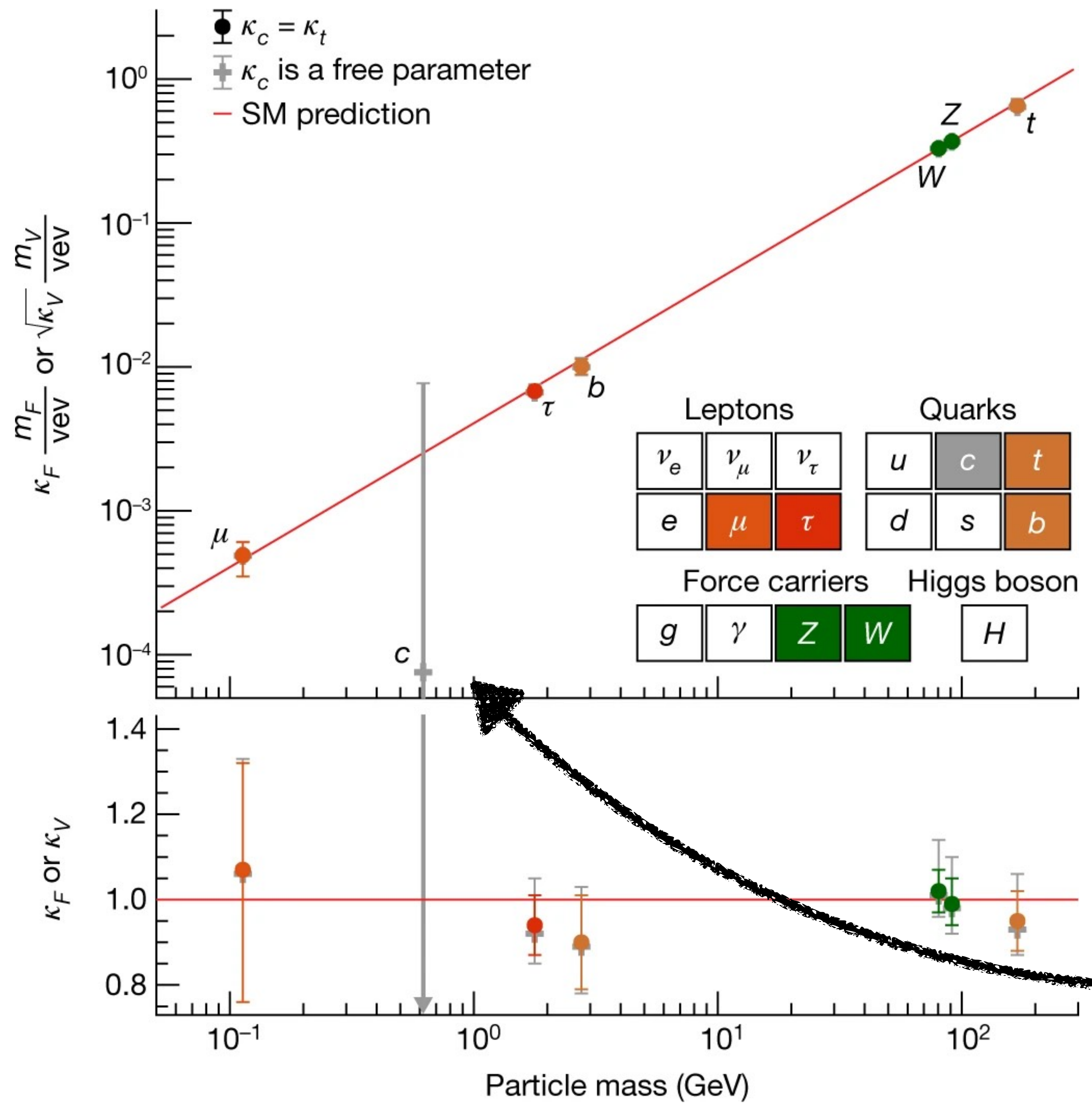

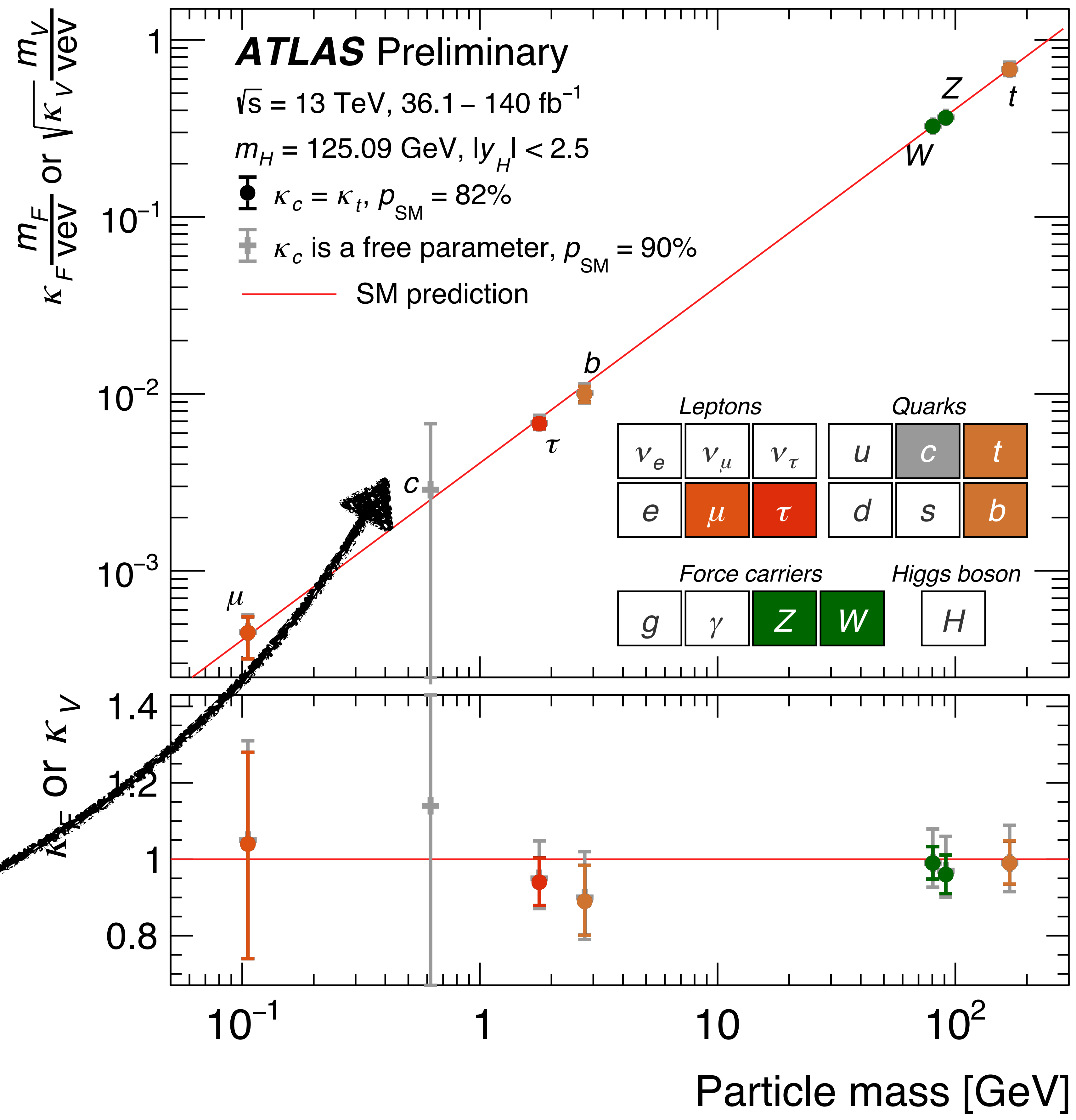

2x improvement in κ_c
(Re-analysis of $H \to cc, bb$)

A new Higgs Boson combination analysis

CONF-2025-006
New for EPS-HEP!

Testing the Yukawa mechanism with improved precision

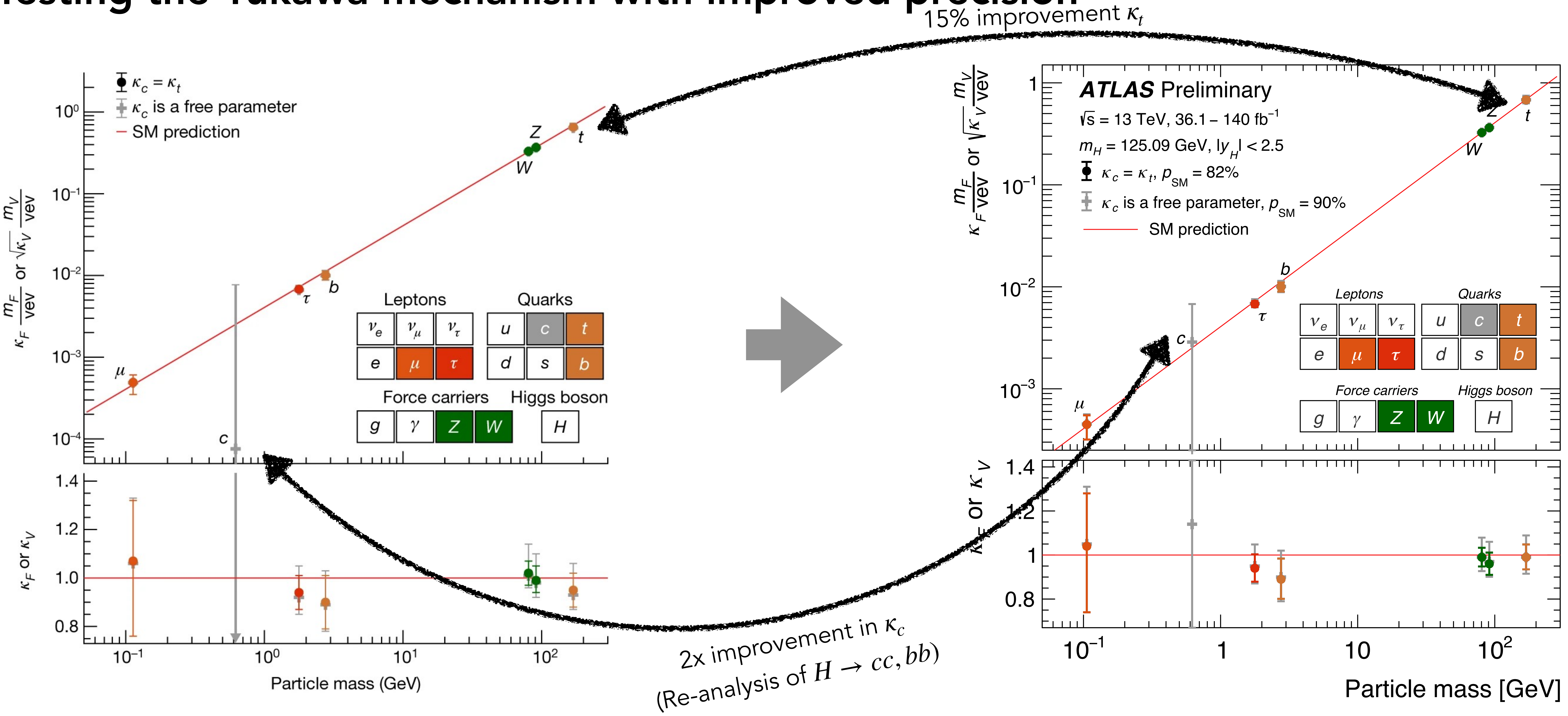

Zooming in:
Higgs to (vector) bosons

Zooming in on (vector) bosons

- Higgs to vector bosons (WW and ZZ) not the largest branching ratio, but relatively clean due to leptonic final states
- Especially the ZZ decay mode is clean due to possibility of no missing energy in the four-lepton final state (4l)
  - Higgs discovery ("golden") channel: $H \rightarrow ZZ^* \rightarrow 4\ell$

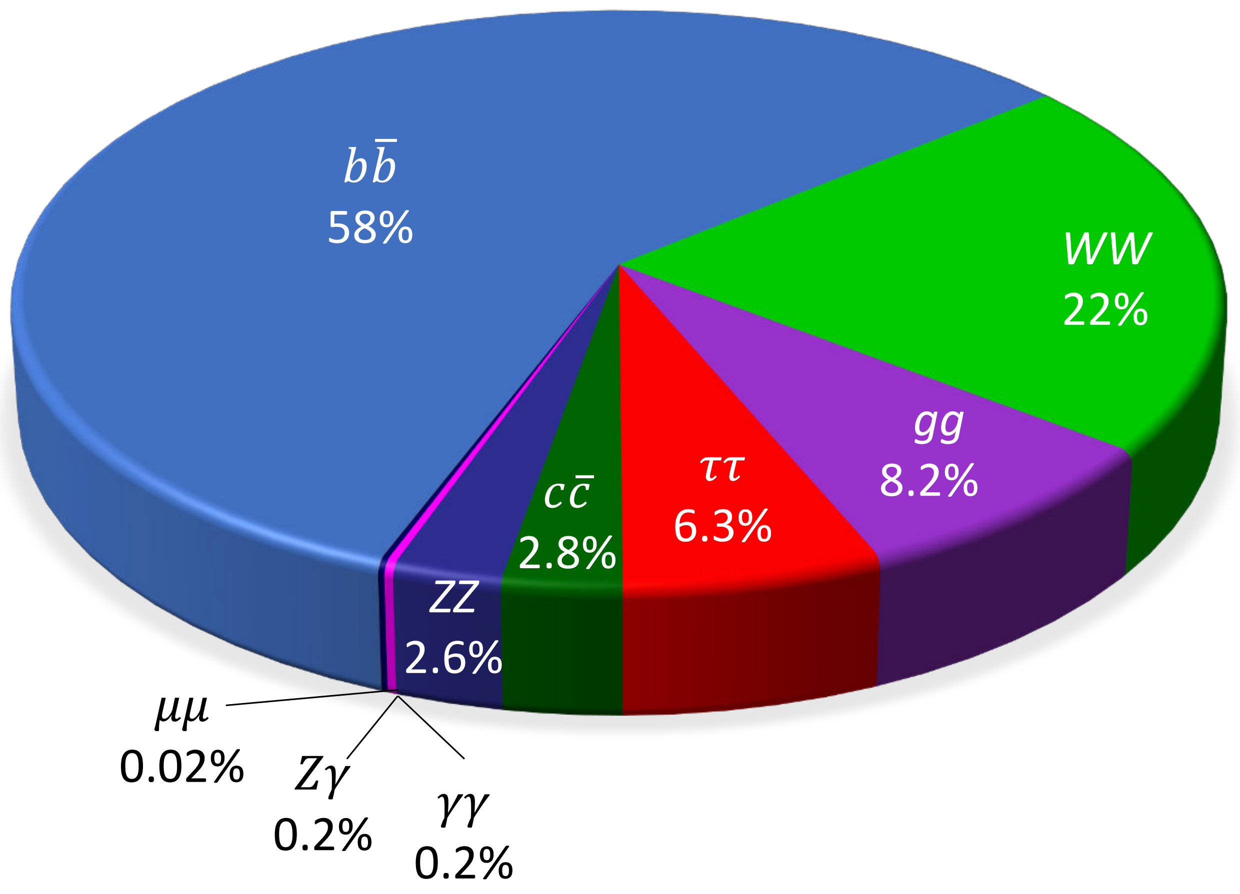

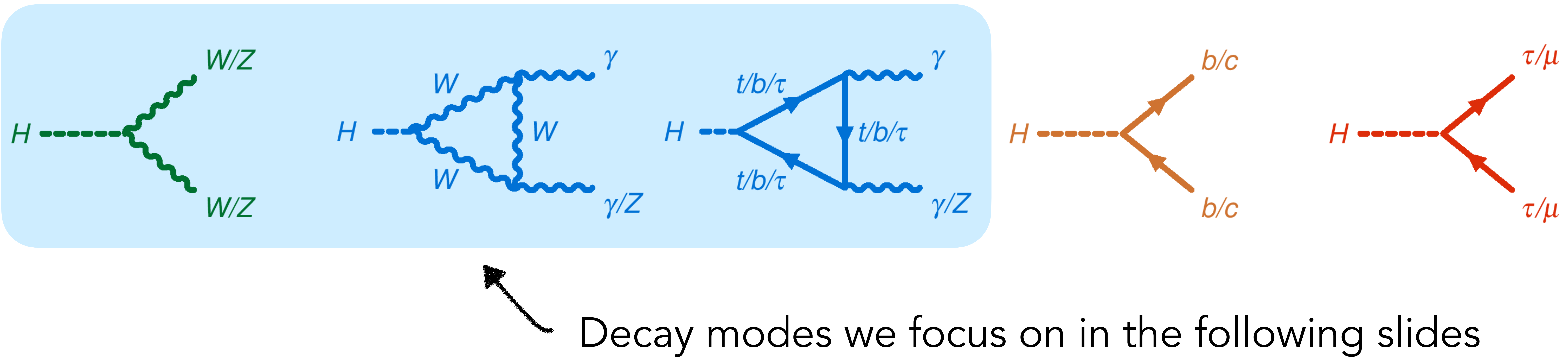

Decay modes we focus on in the following slides

ggF and VBF $H \to WW^*$ measurement at 13 TeV

HIGP-2024-07

Aim:

- Measure the **ggF and VBF signal strengths in Simplified Template Cross Section (STXS) bins, and Effective Field Theory (EFT) interpretation**

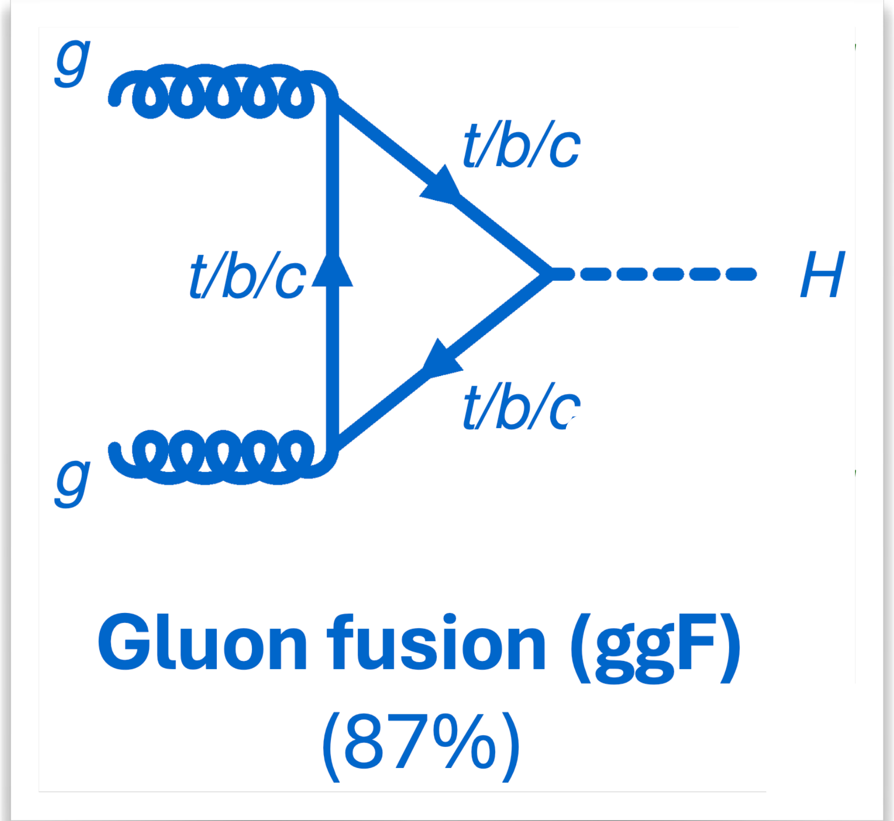

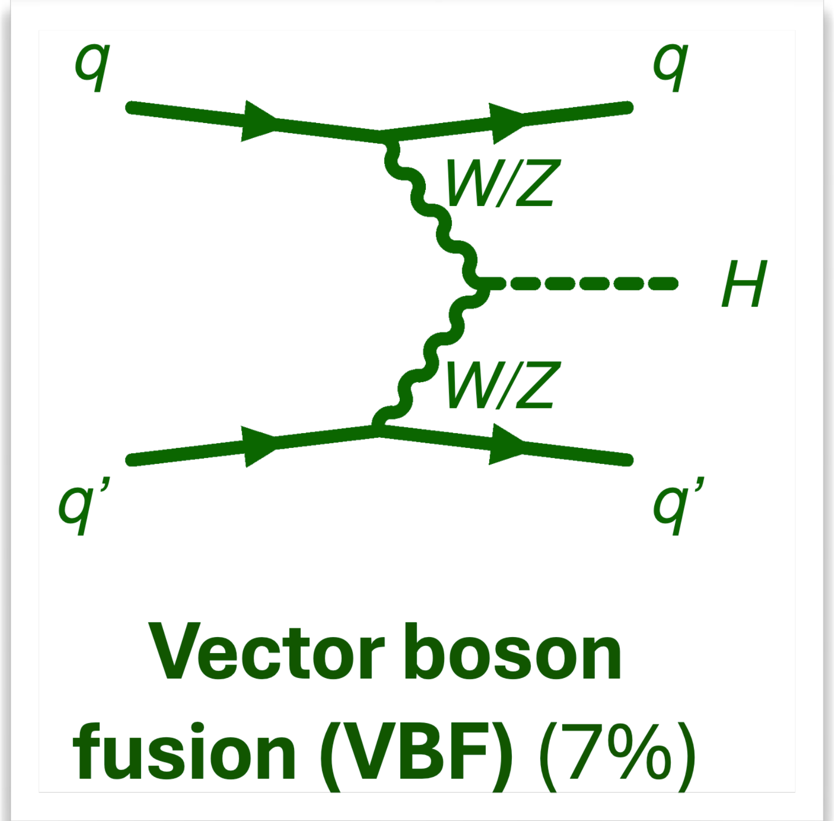

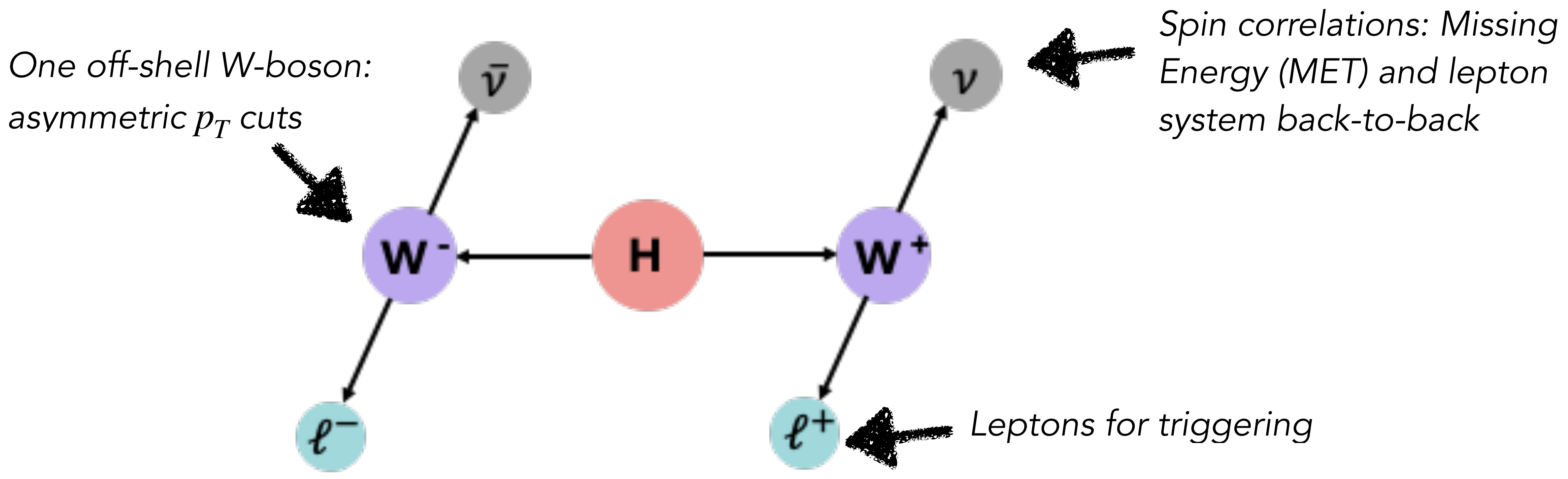

Strategy:

- Target different flavour (DF, $e\nu\mu\nu$) and same flavour (SF, $e\nu e\nu/\mu\nu\mu\nu$) final states
- Categorize events into STXS bins

Multiple improvements since first Run 2 analysis (Phys. Rev. D 108, 032005, 2023):

- Addition of SF channels in stat-limited high p_T^H regions, DNNs as discriminants

ggF and VBF $H \rightarrow WW^*$ measurement at 13 TeV

Results (highlights)

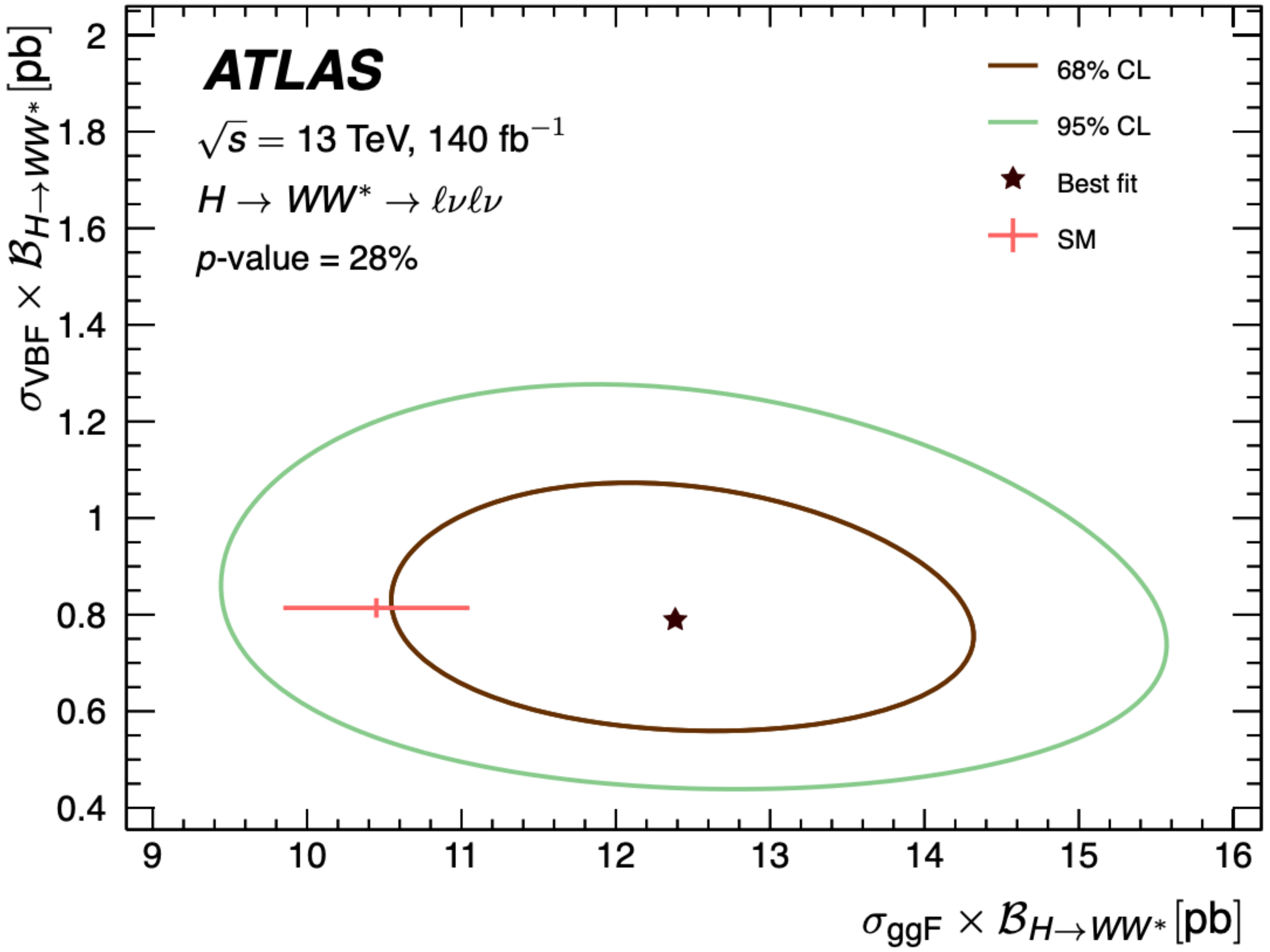

2 Parameter of Interest (POI) fit measuring both production modes ggF and VBF

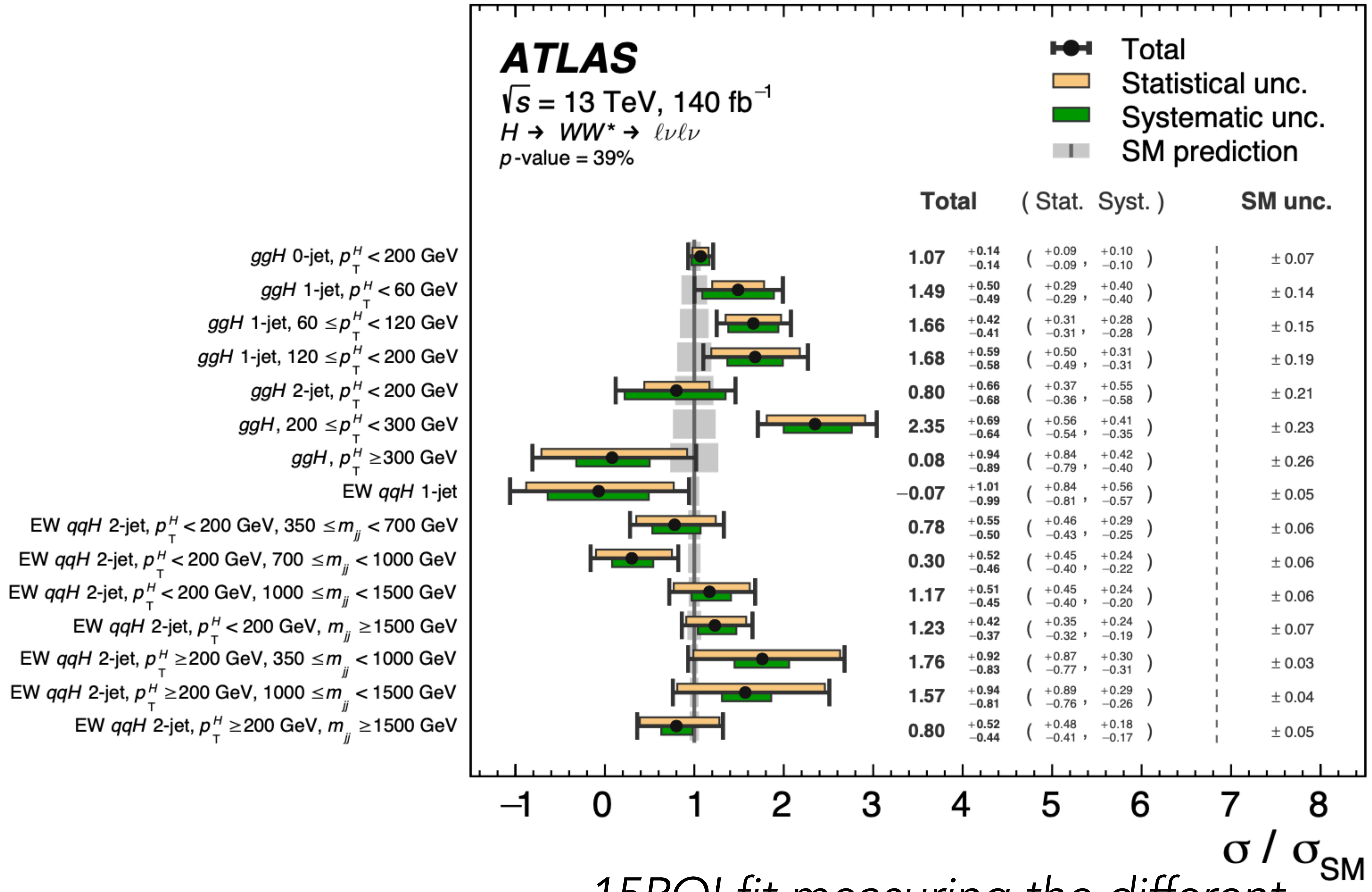

15POI fit measuring the different STXS regions

Results align with standard model predictions!

VH $H \to WW^*$ measurement at 13 TeV

HIGG-2023-09

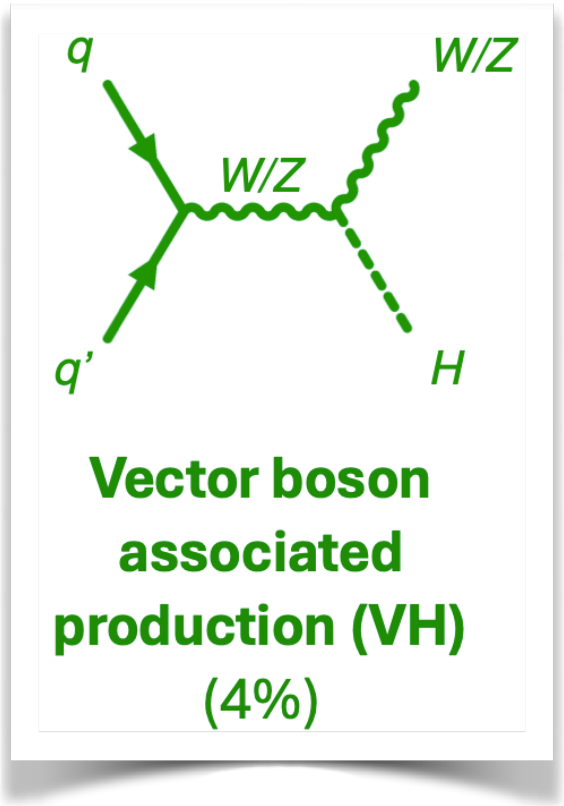

After ggF and VBF, the third most dominant decay mode is VH

- This analysis measures inclusive and STXS VH production in $H \to WW^*$

Strategy

- Target hadronic and leptonic V-decays, split by final state:
  - same-sign (SS) 2ℓ, targeting WH
  - opposite-sign (OS) 2ℓ, targeting VH in general
  - 3ℓ, targeting WH
  - 4ℓ, targeting ZH

- DNN discriminants used in every analysis channel
  - Output nodes for both signals and main backgrounds

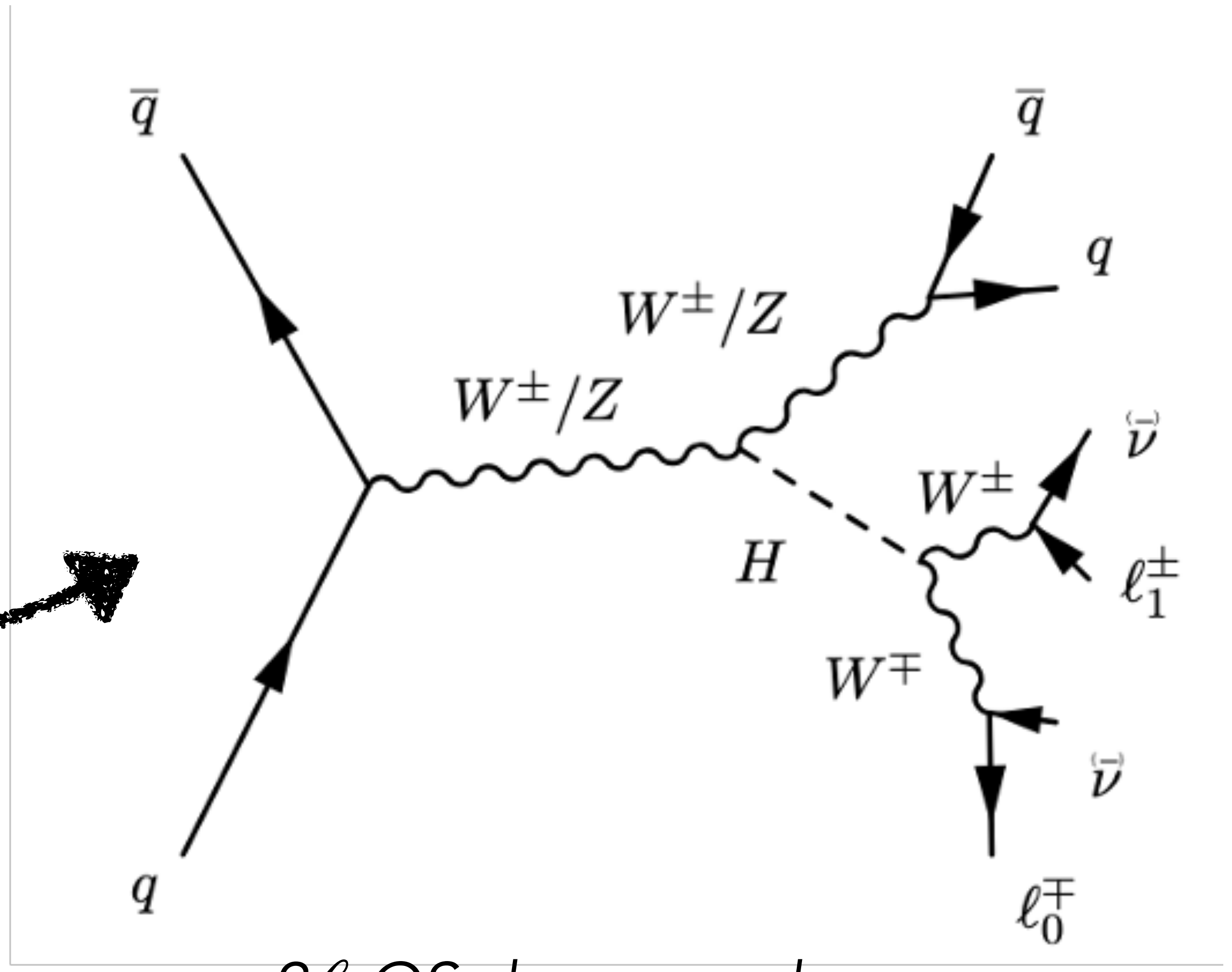

2ℓ OS decay mode

VH $H \to WW^*$ measurement at 13 TeV

HIGG-2023-09

Results (highlights)

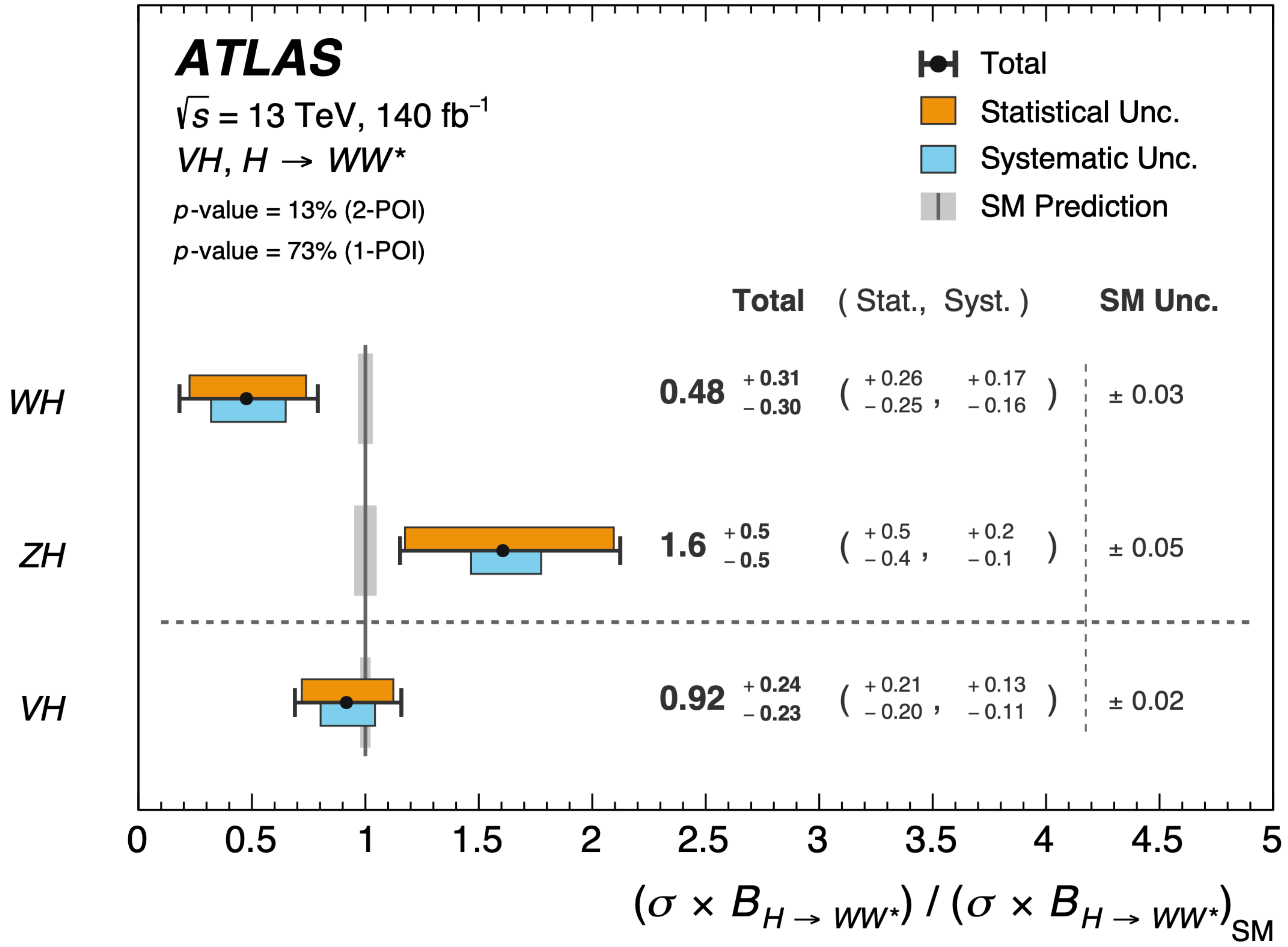

2 POI fit measuring both WH and ZH and their combination into VH production

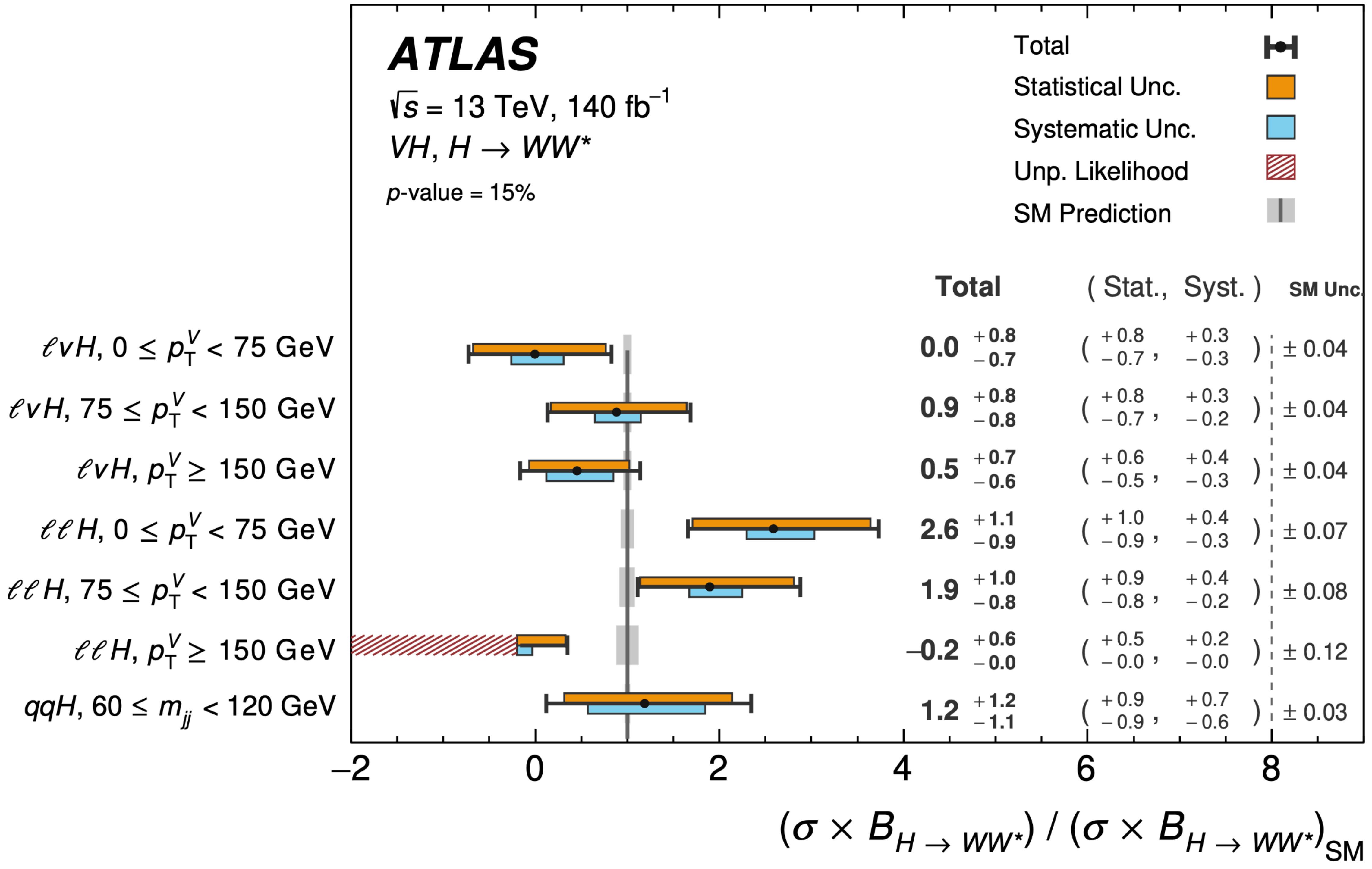

7 POI fit into STXS bins as a function of the momentum of the associated vector boson (p_T^V) → ***Most sensitive low p_T^V VH measurement in ATLAS!***

Recent run 3 results

Interesting channels $H \to ZZ^* \to 4\ell$ and $H \to \gamma\gamma$

- Not the largest BRs, but the **cleanest Higgs decay channels**, making them **interesting for early Run 3 results!**

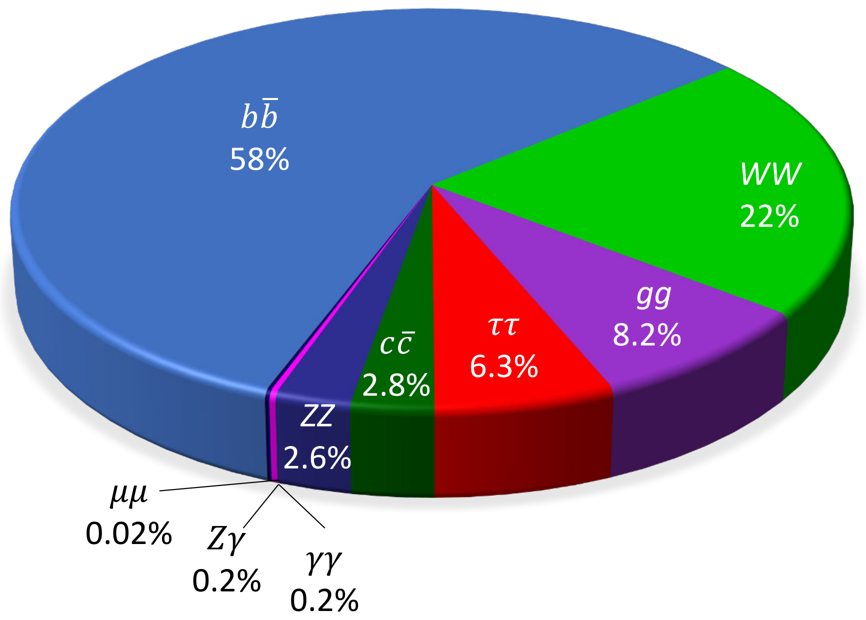

Electrons and muons leave tracks and calo deposits

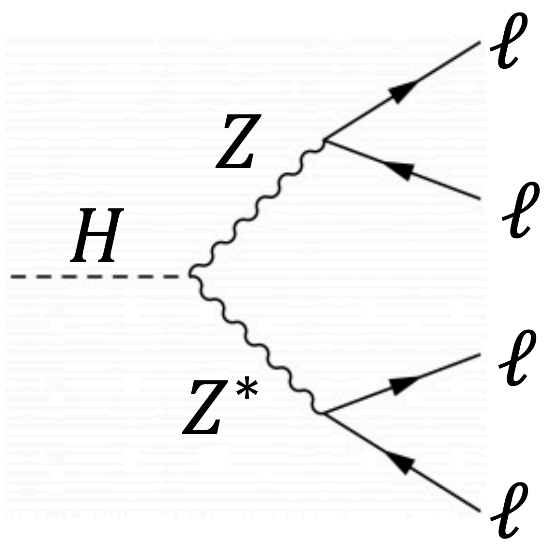

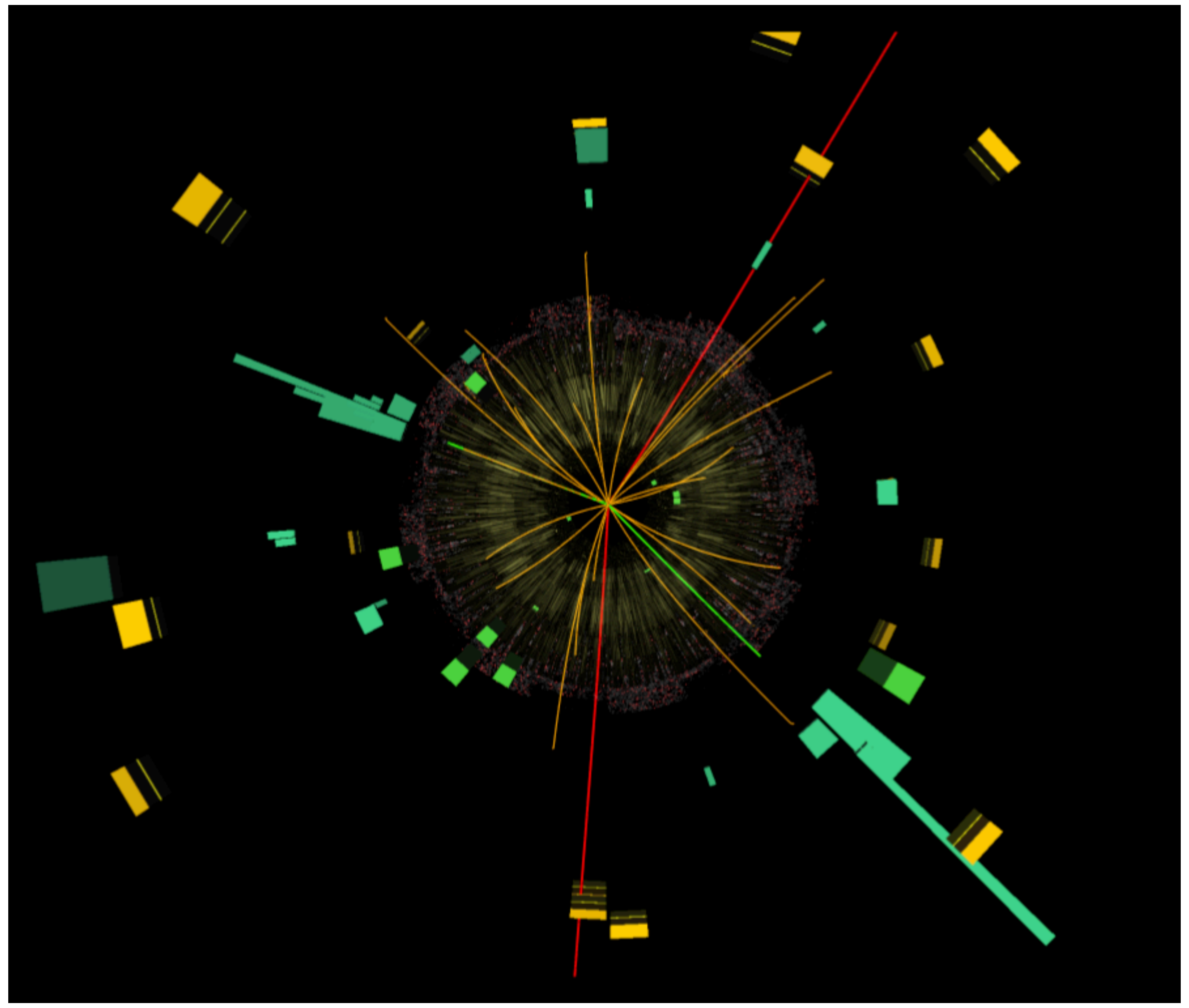

$H \to ZZ^* \to 4\ell$

Photons leave calo deposits

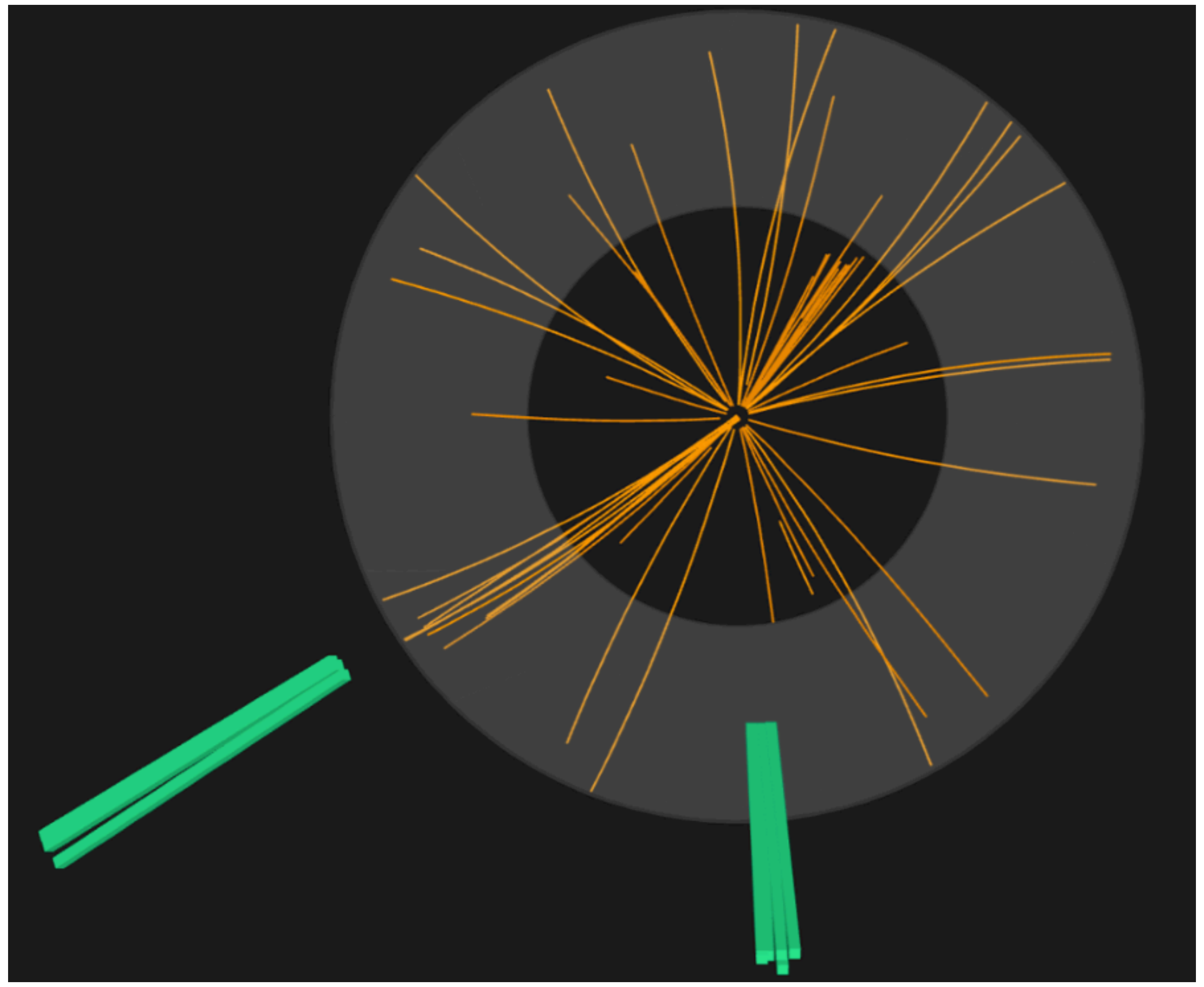

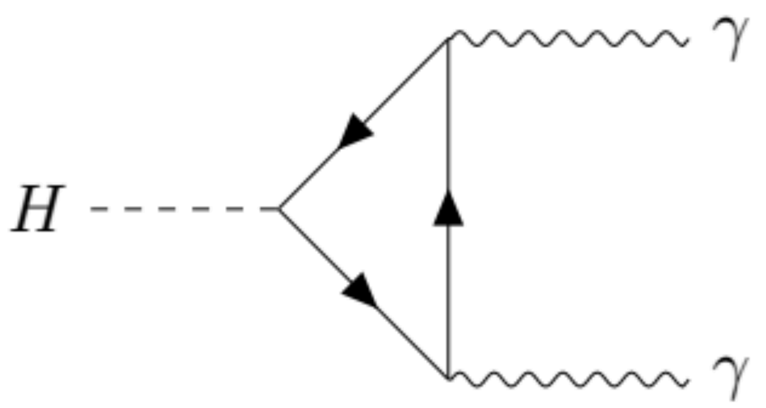

$H \to \gamma\gamma$

$H \to ZZ^* \to 4\ell$ + $H \to \gamma\gamma$ at 13.6 TeV

Eur. Phys. J. C 84 (2024) 78

Aim:

LHC Run 3 collision energy!

- Measure 13.6 TeV cross section of inclusive Higgs production, $\sigma(pp \to H)$, using Run 3 2022 dataset

Strategy:

- **Measure a fiducial phase space** for both decay modes via a fit to the invariant mass spectra → extrapolate to inclusive Higgs production using SM branching ratios

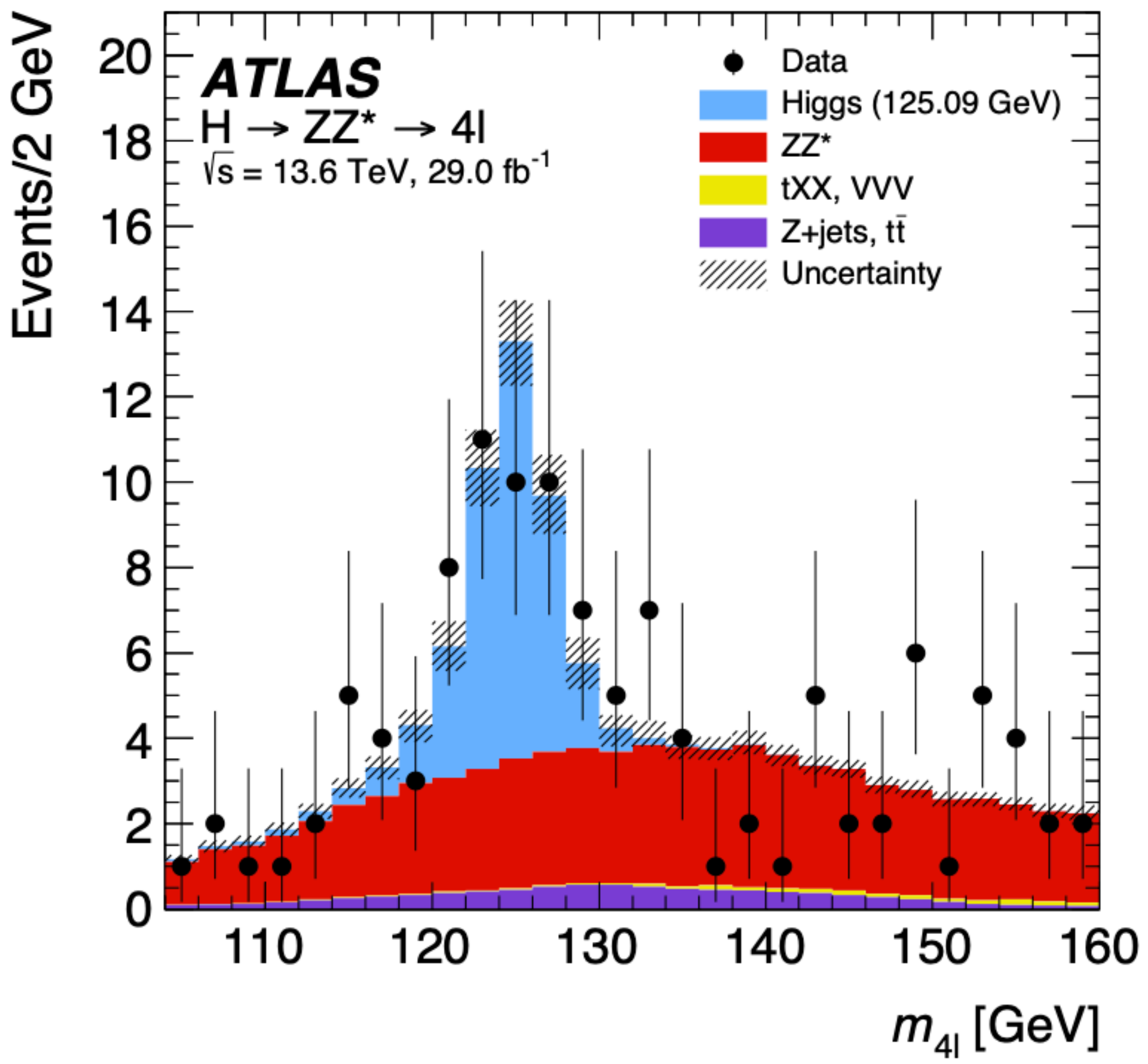

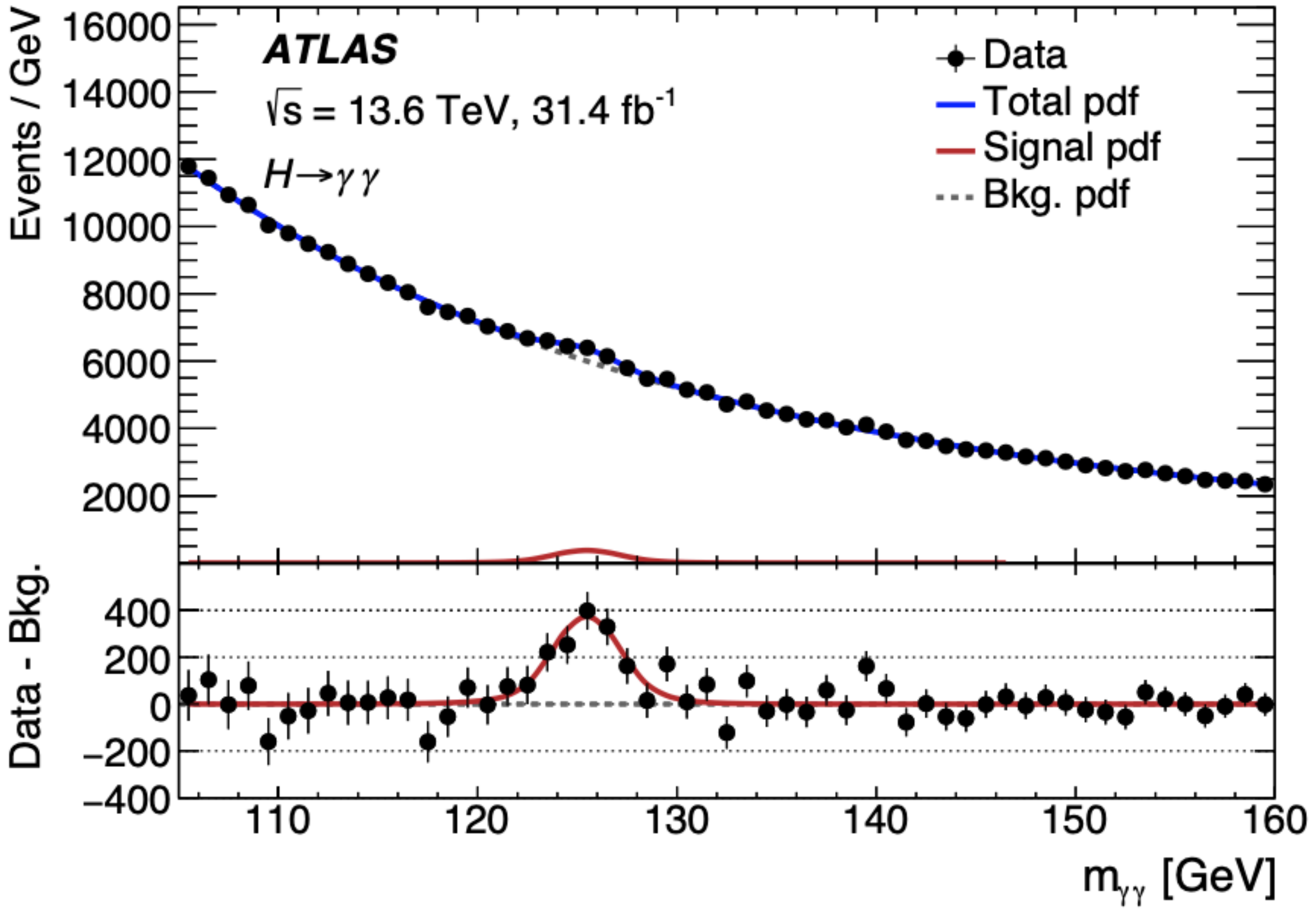

$H \to ZZ^* \to 4\ell$ + $H \to \gamma\gamma$ at 13.6 TeV

Eur. Phys. J. C 84 (2024) 78

- **Below are results as a function of the LHC collision energy across the different runs,** observed trend follows standard model very well!

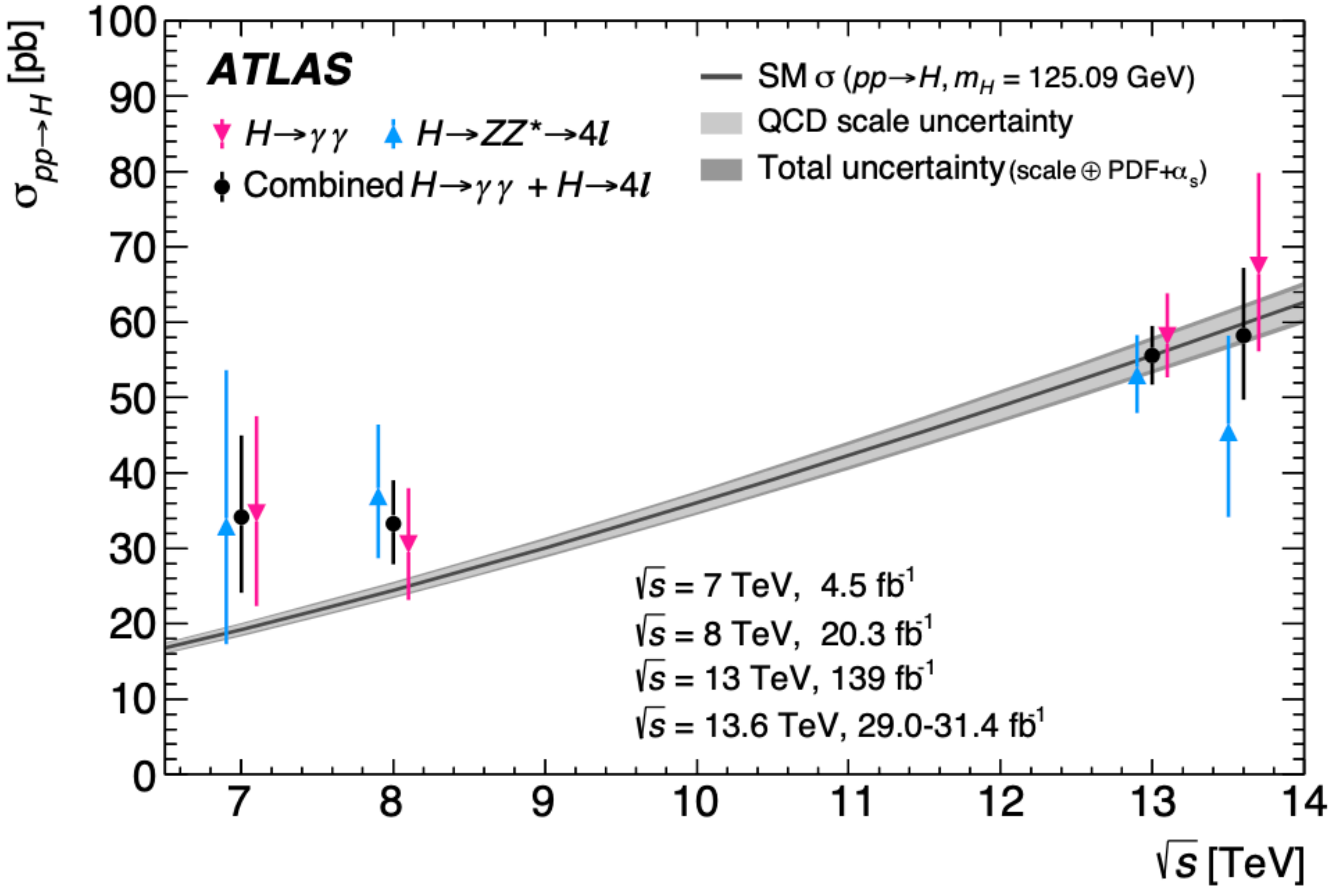

$$\sigma(pp \to H)_{\text{obs.}} = 58.2 \ \pm \ 8.7 \text{ pb}$$

$$\sigma(pp \to H)_{\text{SM}} = 59.9 \ \pm \ 2.6 \text{ pb}$$

- Uncertainties dominated by **statistical components** for both analyses
- For diphoton analysis **photon reconstruction** and **spurious signal uncertainty** play a significant role as well

More data for $H \to ZZ^* \to 4\ell$ at 13.6 TeV

CONF-HIGP-2024-22

- An extended analysis of $H \to ZZ^* \to 4\ell$ adding an extra year of data-taking at 13.6 TeV, 56 fb^{-1} total

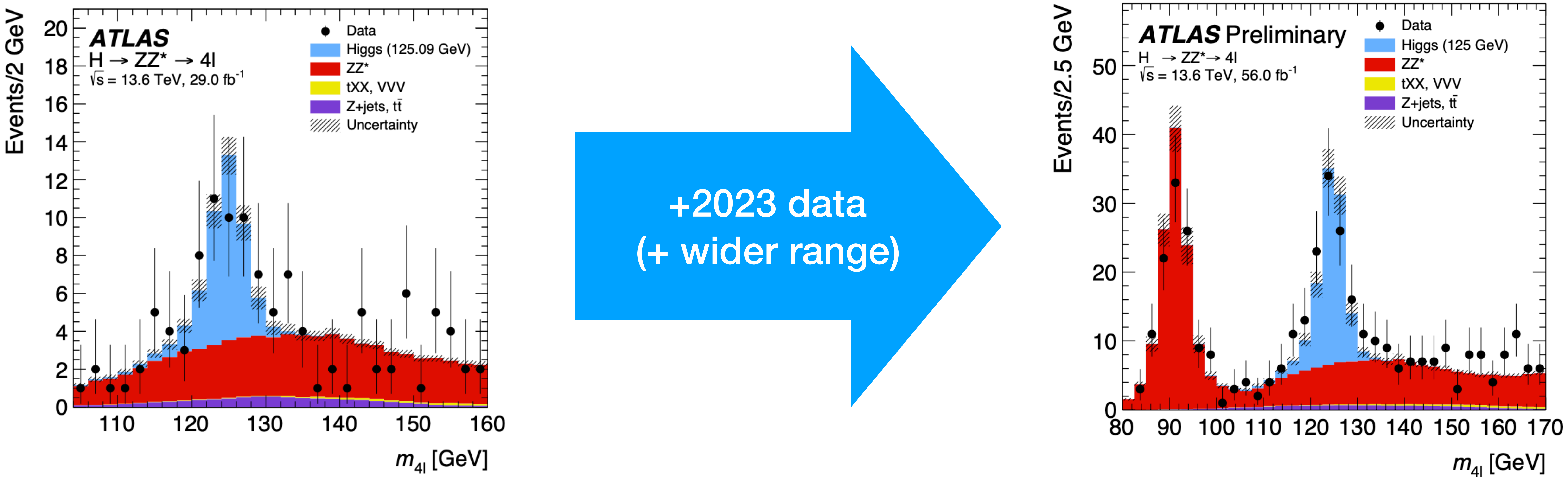

Aim: To measure the following quantities, on top of the fiducial cross-section:

- differential cross sections ($p_T^{4\ell}$, $y_{4\ell}$, N_{jets}, m_{34})
- **production mode cross sections (ggF, VBF, VH, and ttH), for the first time at 13.6 TeV!**
- Coupling strength parameters in the κ framework
- Wilson coefficients of the effective field theory (SMEFT) framework

More data for $H \rightarrow ZZ^* \rightarrow 4\ell$ at 13.6 TeV

Results (highlights)

Statistical combination of run 2 and run 3 datasets!

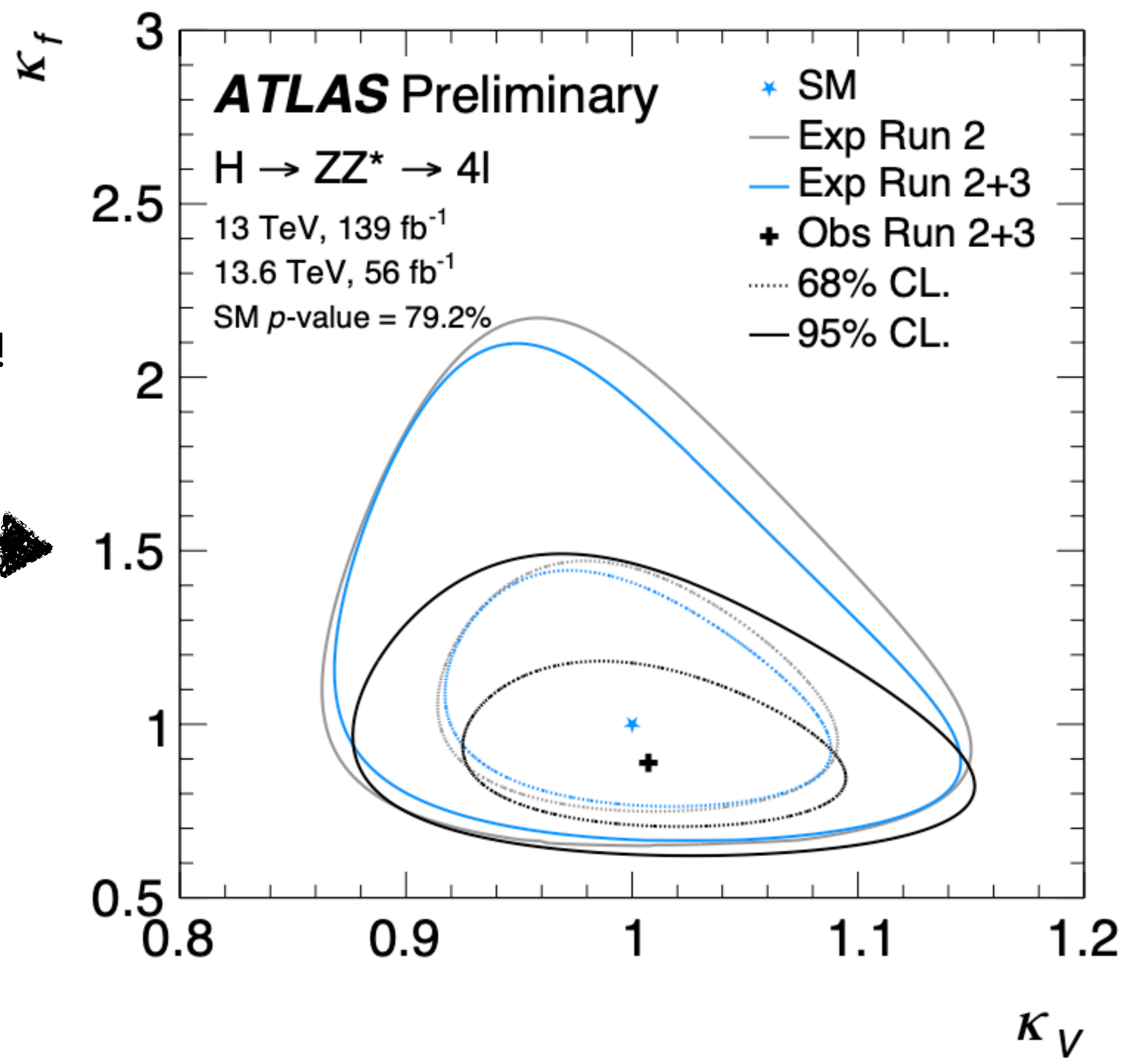

Higgs to fermion and Higgs to vector boson coupling strength modifiers from STXS measurement!

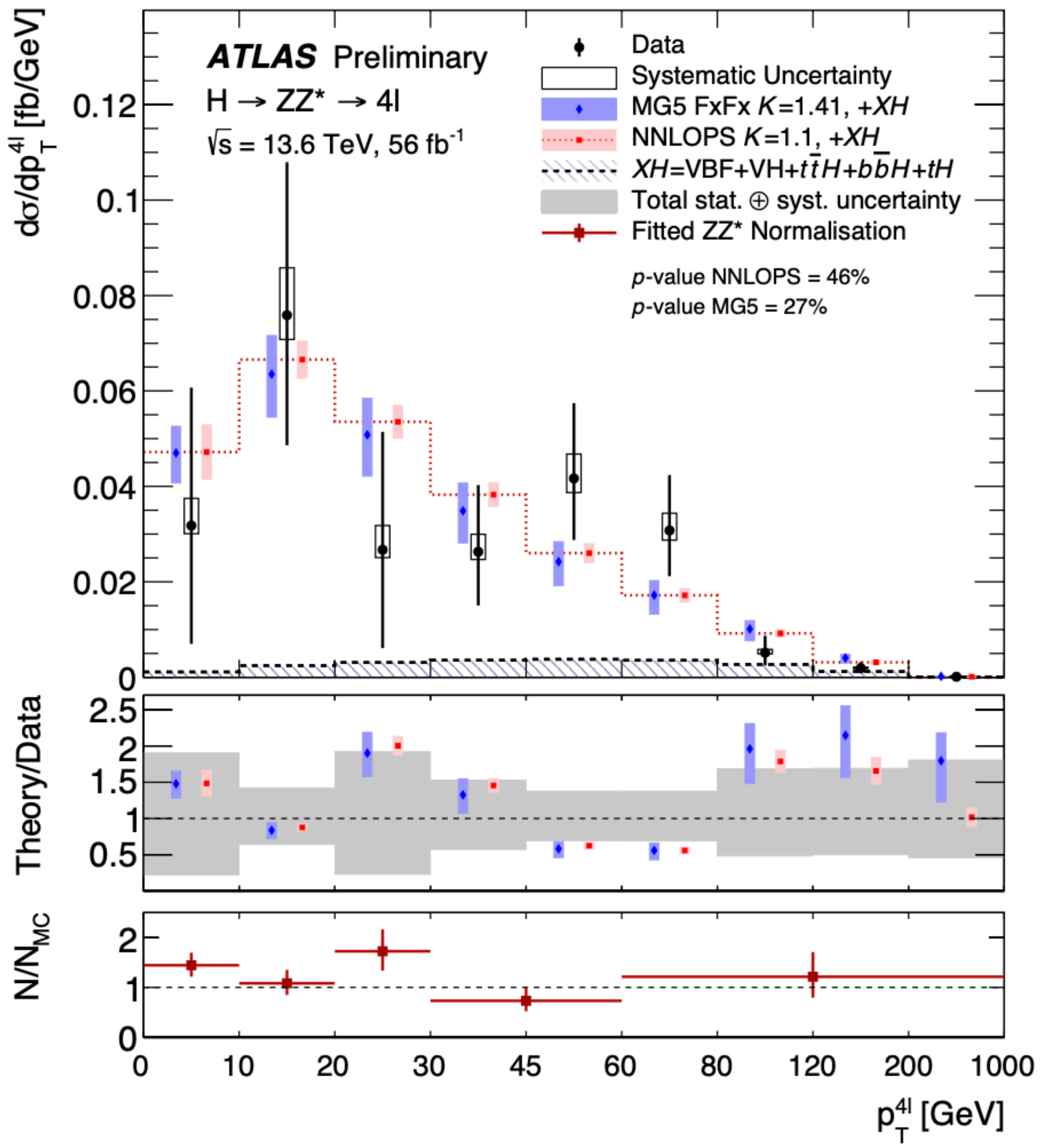

Differential measurement of $p_T^{4\ell}$

Conclusion

ATLAS is **consolidating results from LHC Run 2**

- Updates to $H \to WW^*$ via VH, ggF, and VBF production modes
- Presented for the first time improved Higgs global combination ("legacy Run 2") results!

The ATLAS LHC **Run 3 physics programme is ramping up** with sensitive measurements in the H to ZZ^* and $\gamma\gamma$ decay modes

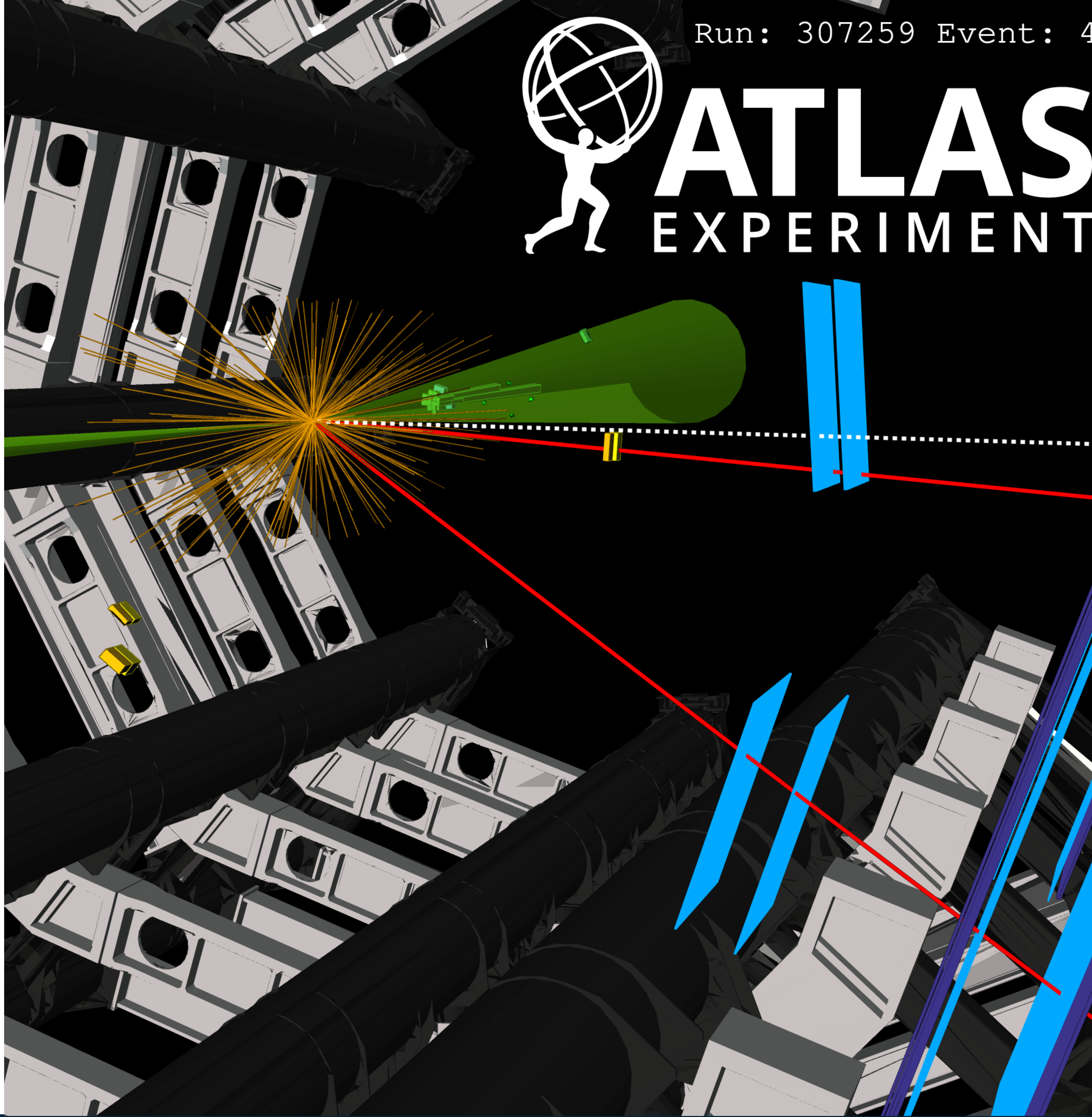

Backup

$H \to ZZ \to 4\ell$ + $H \to \gamma\gamma$ at 13.6 TeV uncertainty breakdown

Source	Uncertainty [%]
Statistical uncertainty	25.1
Systematic uncertainty	7.9
Electron uncertainties	6.3
Muon uncertainties	3.8
Luminosity	2.2
ZZ^* theoretical uncertainties	0.7
Reducible background estimation	0.6
Other uncertainties	<1.0
Total	26.4

$H \to ZZ \to 4\ell$

Source	Uncertainty [%]
Statistical uncertainty	14.0
Systematic uncertainty	10.3
Background modelling (spurious signal)	6.0
Photon trigger and selection efficiency	5.8
Photon energy scale & resolution	5.5
Luminosity	2.2
Pile-up modelling	1.2
Higgs boson mass	0.1
Theoretical (signal) modelling	<0.1
Total	17.4

$H \to \gamma\gamma$

$H \to ZZ \to 4\ell$ + $H \to \gamma\gamma$ at 13.6 TeV fiducial regions

Leptons	
Leptons	$p_T > 5$ GeV, $\|\eta\| < 2.7$
Lepton selection and pairing	
Lepton kinematics	$p_T > 20, 15, 10$ GeV
Leading pair (m_{12})	SFOC lepton pair with smallest $\|m_Z - m_{\ell\ell}\|$
Subleading pair (m_{34})	remaining SFOC lepton pair with smallest $\|m_Z - m_{\ell\ell}\|$
Event selection (at most one quadruplet per event)	
Mass requirements	50 GeV $< m_{12} < 106$ GeV and 12 GeV $< m_{34} < 115$ GeV
Lepton separation	$\Delta R(\ell_i, \ell_j) > 0.1$
J/ψ veto	$m(\ell_i, \ell_j) > 5$ GeV for all SFOC lepton pairs
Mass window	105 GeV $< m_{4\ell} < 160$ GeV
If extra lepton with $p_T > 12$ GeV	quadruplet with largest matrix element value

Photons	
Leading (sub-leading) p_T^γ	$p_T^\gamma / m_{\gamma\gamma} > 0.35(0.25)$
Pseudorapidity	$\|\eta\| < 2.37$ and outside $1.37 < \|\eta\| < 1.52$
Isolation ($\Delta R = 0.2$)	$E_T^{iso} / E_T^\gamma < 0.05$
Di-photon system	
Mass window	105 GeV $< m_{\gamma\gamma} < 160$ GeV

$H \to ZZ \to 4\ell$

$H \to \gamma\gamma$

$H \rightarrow ZZ \rightarrow 4\ell$ + $H \rightarrow \gamma\gamma$ at 13.6 correlation scheme

Experimental and theoretical uncertainties that affect both channels are correlated via common nuisance parameters. The correlated experimental uncertainties include the uncertainties in the integrated luminosity, in the description of pile-up in the simulation, in the common electron–photon energy scale, in the Higgs boson mass value, and in the relative contributions of the different Higgs boson production modes. Additionally, the common sources of theoretical uncertainty in the $H \rightarrow ZZ^* \rightarrow 4\ell$ and $H \rightarrow \gamma\gamma$ branching fractions (α_s, b- and c-quark masses, and partial decay widths into the main decay channels, such as two vector bosons, two gluons, or a $b\bar{b}$ pair) are also correlated. Finally, the theoretical uncertainties in the acceptance factor due to missing higher-order QCD effects, PDF variations, variations of the modelling of the PS, and signal composition are also correlated.

$H \to ZZ \to 4\ell$ at 13.6 TeV

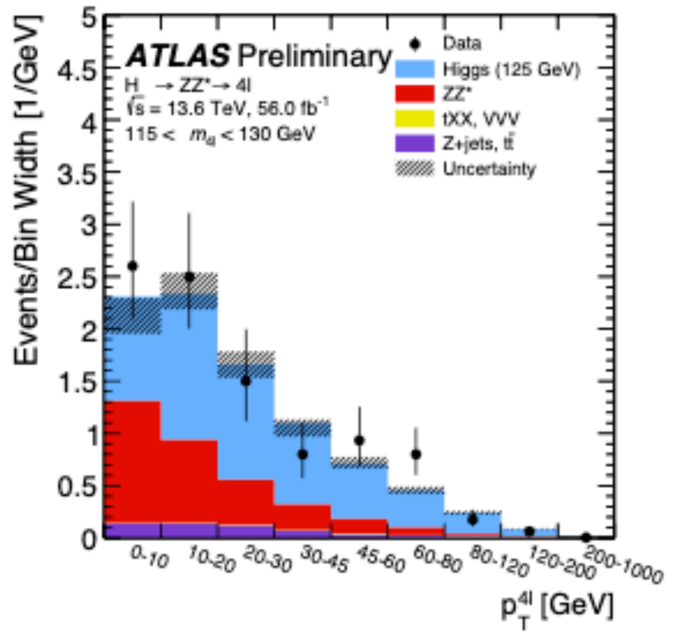

(a) $p_T^{4\ell}$

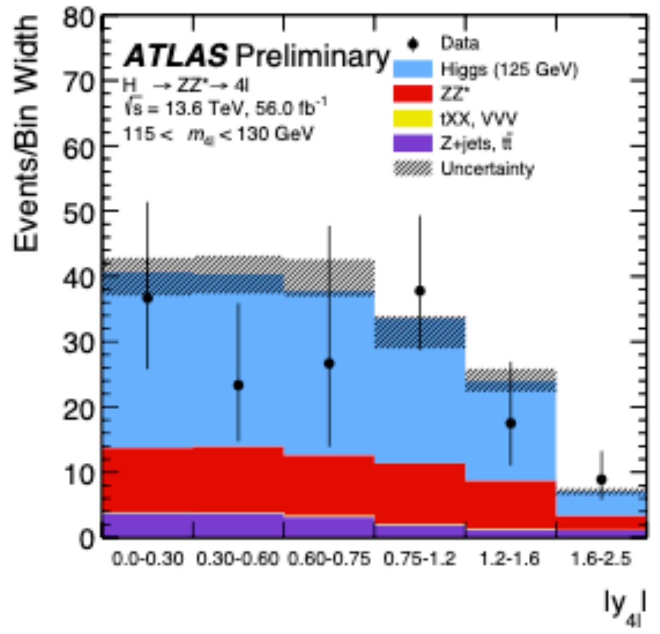

(b) $|y_{4\ell}|$

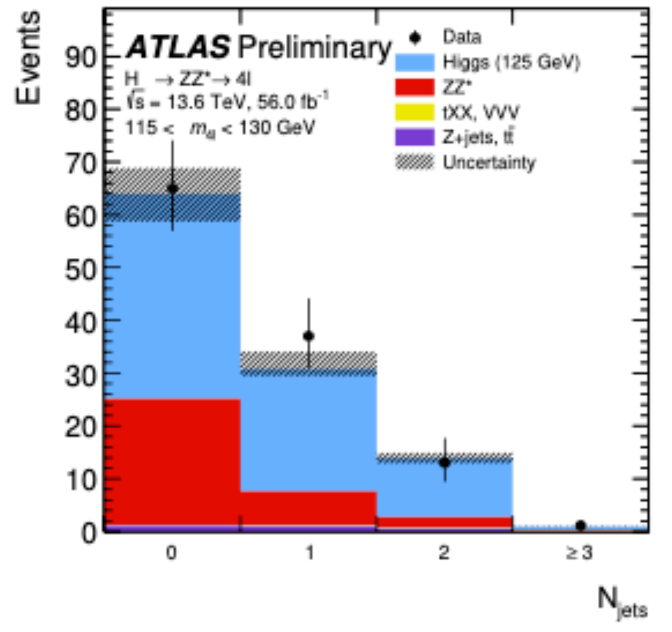

(c) N_{jets}

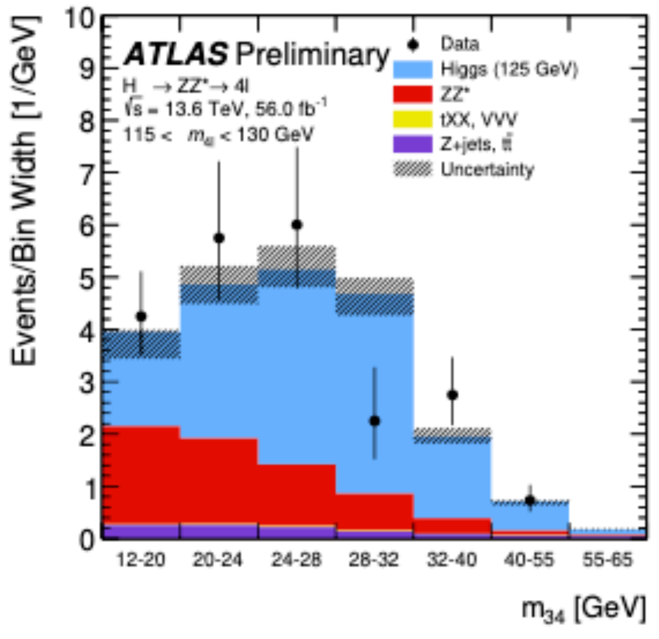

(d) m_{34}

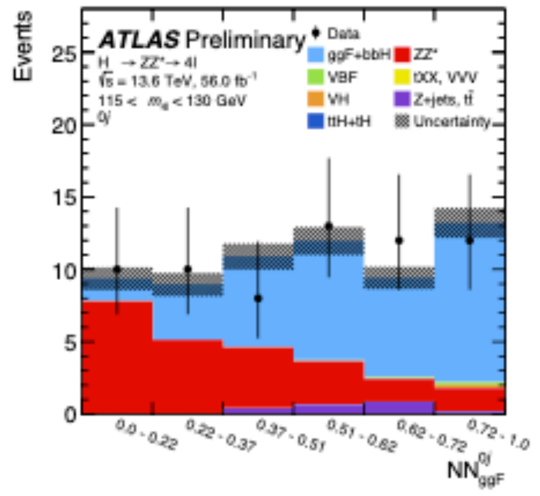

(a) $0j$

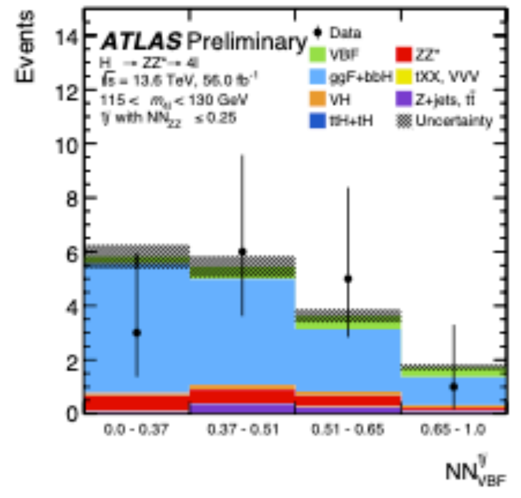

(b) $1j$ ($\text{NN}_{ZZ} \leq 0.25$)

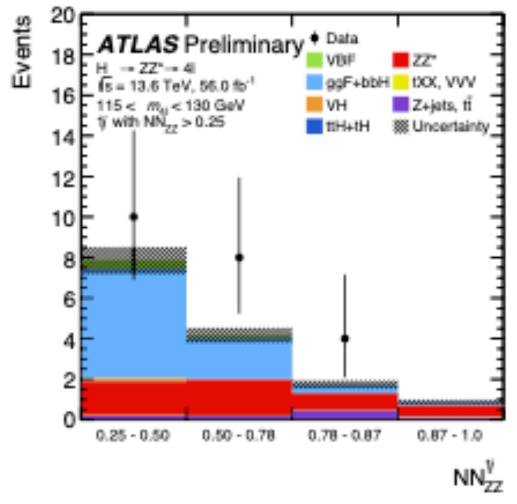

(c) $1j$ ($\text{NN}_{ZZ} > 0.25$)

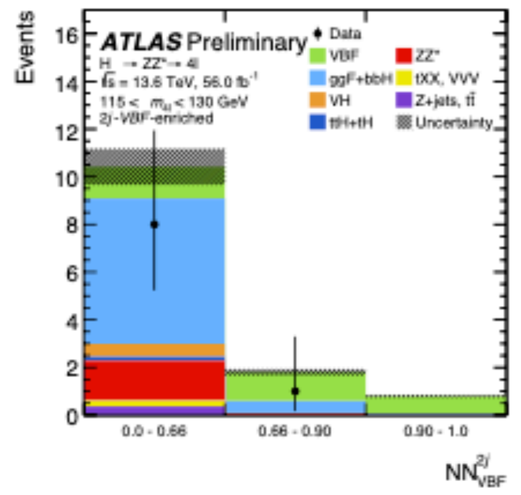

(d) $2j$-VBF-enriched

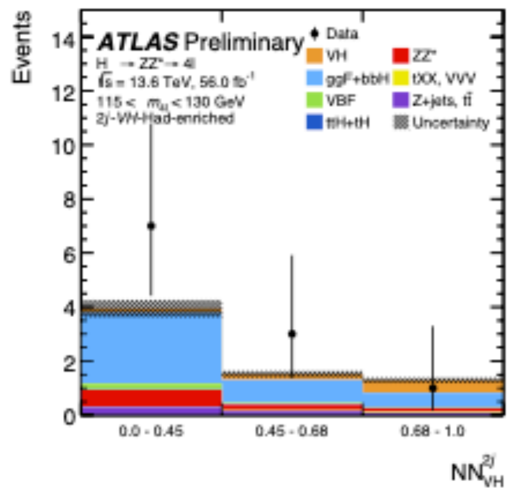

(e) $2j$-VH-Had-enriched

Wilson coefficient	Expected 68% CL	Expected 95% CL	Observed 68% CL	Observed 95% CL	Best-fit value
c_{HW}	[−1.2, 1.4]	[−2.1, 2.3]	[−1.7, 1.5]	[−2.8, 2.7]	−0.9
c_{HB}	[−0.4, 0.4]	[−0.7, 0.6]	[−0.6, 0.5]	[−0.9, 0.7]	−0.3
c_{HWB}	[−0.9, 0.7]	[−1.3, 1.1]	[−1.0, 0.9]	[−1.5, 1.4]	0.5

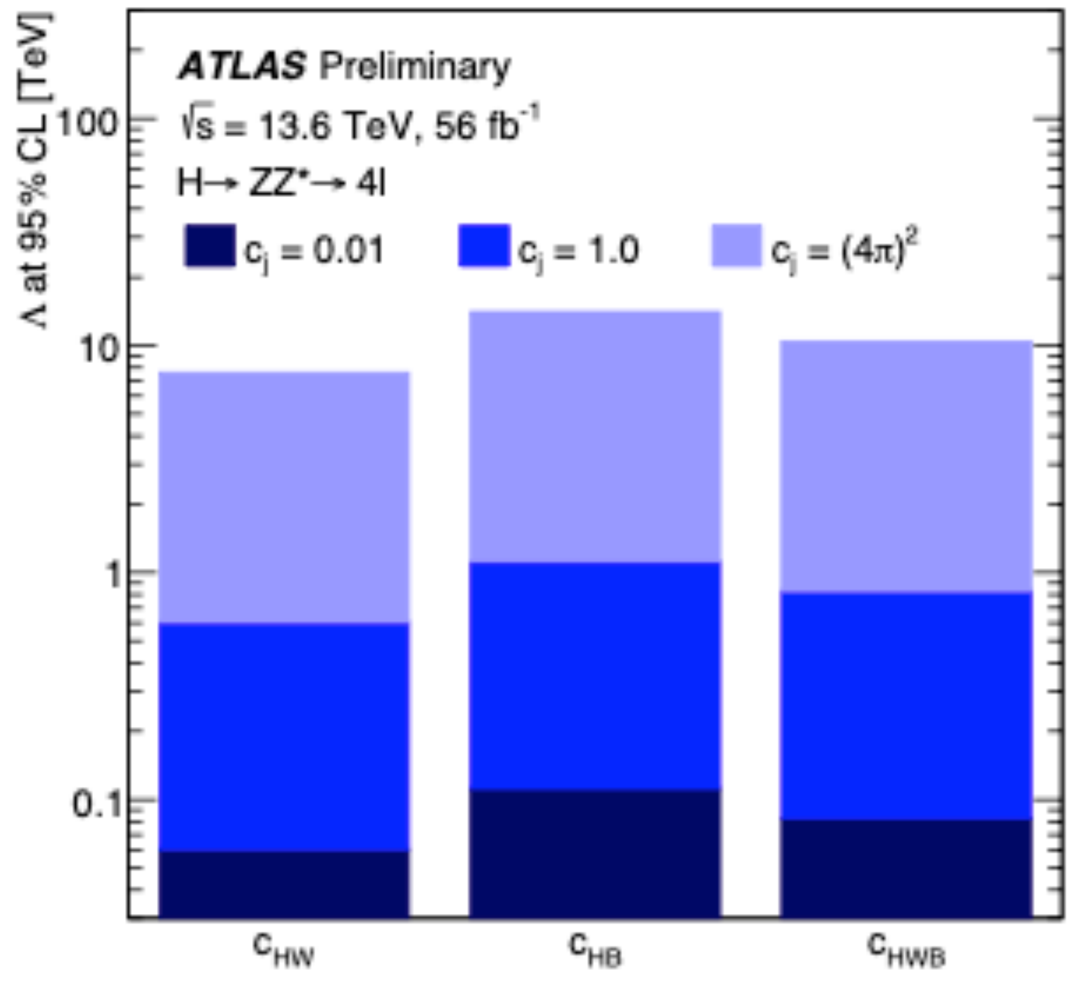

accounting for systematic uncertainties introduced in Section 7. The following experimental uncertainties from both measurements are treated as correlated: muon transverse momentum scale and reconstruction efficiency; electron energy scale and energy resolution; jet energy scale and resolution, except for additional Run 3 specific uncertainty contributions. Other uncertainties are treated as uncorrelated in the fit: luminosity, electron and photon efficiency; jet flavour response, missing transverse energy and jet pileup tagging and jet flavour identification. Theoretical uncertainties arising from missing higher order corrections on the Higgs signal cross-sections in exclusive kinematic regions; shifts in Higgs mass, and on background estimates are correlated. All other theory uncertainties, including PDF and parton shower variations, are uncorrelated.

Stat. dominated, other important uncertainties come from lepton reco and isolation efficiencies,
and jet energy scale measurements (for N_jets)

inclusive in the final states and Higgs boson production modes. The Higgs boson transverse momentum $p_T^{4\ell}$ provides a test of perturbative QCD calculations and is sensitive to the structure of the Higgs boson interactions. The rapidity of the Higgs boson $y_{4\ell}$ is sensitive to the parton distribution functions for the colliding protons, and is also influenced by QCD radiative corrections. The jet multiplicity N_{jets} is sensitive to different production mechanisms and provides sensitivity to the theoretical modeling of high-p_T quark and gluon emission. Finally, the invariant mass of the sub-leading lepton pair m_{34} is sensitive to higher-order electroweak corrections to the Higgs boson decay and probes the BSM contributions in the HZZ interaction vertex. The total cross section is determined from the inclusive fiducial cross section

$H \to ZZ \to 4\ell$ at 13.6 TeV

Process	Cross-section accuracy	Cross-section value
ggF	N3LO QCD + NLO EW	52.17 pb
VBF	NNLO QCD + NLO EW	4.075 pb
WH	NNLO QCD + NLO EW	1.453 pb
ZH	NNLO QCD + NLO EW	0.942 pb
$t\bar{t}H$	NLO QCD + NLO EW	0.569 pb
$b\bar{b}H$	5FS/NNLO + 4FS/NLO QCD	0.525 pb
tH	NLO QCD	0.087 pb
tWH	NLO QCD	0.017 pb

ıble 1: Values and accuracy of the cross-sections used to normalise the Higgs signal processes.

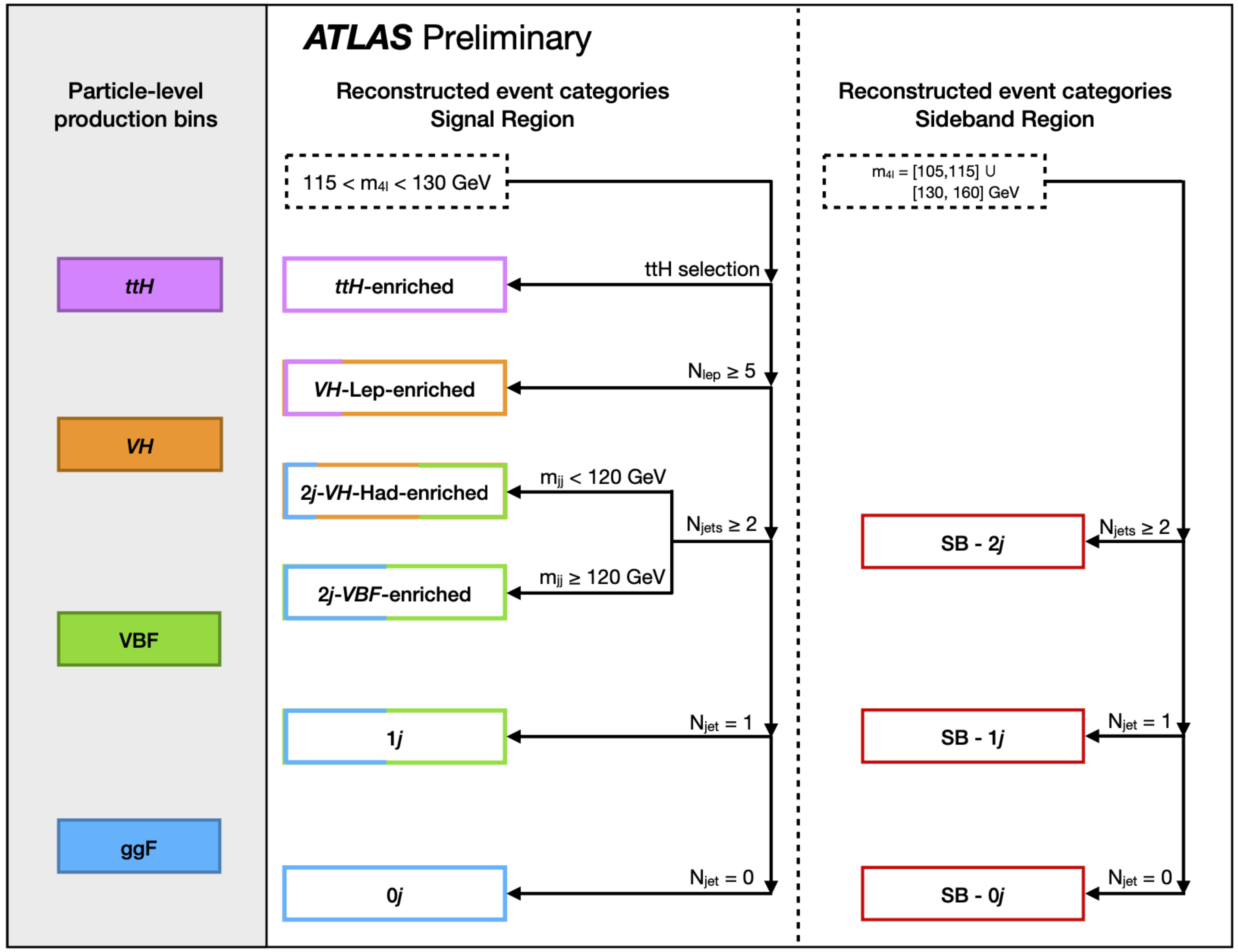

Multivariate discriminants used in each of these

Figure 1: Higgs boson production modes defined at particle-level (left panel), and the corresponding reconstructed event categories for signal (middle panel) and sidebands (right panel). The $b\bar{b}H$ (tH) contribution is considered as a part of the ggF ($t\bar{t}H$) production mode cross-section. The colors of each reconstructed event category box indicate the approximate contributions from the relevant production modes.

VH $H \to WW$ measurement at 13 TeV

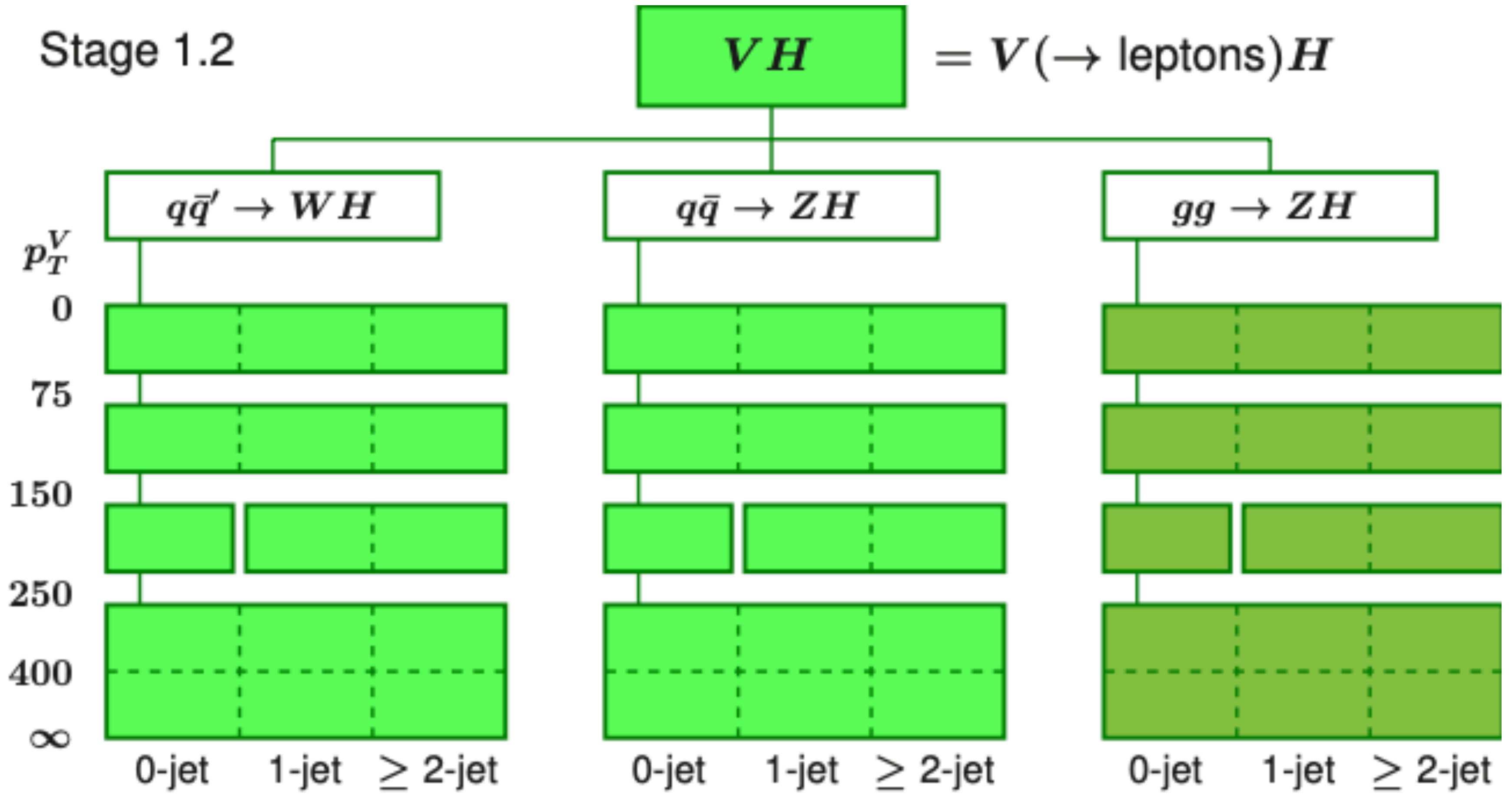

Figure 17: The Stage 1.2 STXS categorisation scheme for VH production [22].

Channel	2ℓ OS	2ℓ SS	3ℓ Z-dominated	3ℓ Z-depleted	4ℓ 1-SFOS	4ℓ 2-SFOS
Minimum lepton p_{T} [GeV]	15	15	15	15	10	10
Number of leptons	2	2	3	3	4	4
Total lepton charge	0	±2	±1	±1	0	0
Number of SFOS pairs	0	–	1 or 2	0	1	2
Number of DFOS pairs	1	–	–	–	–	–
Minimum $\Delta R_{\ell\ell}$	0.1	0.4	0.1	0.1	0.2 ($\ell_0\ell_1$)	
Minimum $m_{\ell\ell}$ [GeV]	10	–	12 (all SFOS)	–	12 (all SFOS) or 10 (all DFOS)	
Number of jets	≥ 2	≥ 1	–	–	–	–
Number of b-tagged jets	0	0	0	0	0	0
$\|m_{\ell\ell} - m_Z\|$ [GeV]	–	> 20 ($e^{\pm}e^{\pm}$)	> 25 (all SFOS)	–	–	–
$m_{\ell\ell}$ [GeV]	–	–	–	–	–	< 50 ($\ell_0\ell_1$)
$E_{\mathrm{T}}^{\mathrm{miss}}$ [GeV]	–	–	> 30	–	–	–
$\|m_{jj} - 85\ \mathrm{GeV}\|$ [GeV]	< 15	–	–	–	–	–
m_{jj} [GeV]	–	< 500	–	–	–	–
Δy_{jj}	< 1.2	–	–	–	–	–
$\|m_{4\ell} - 122.5\ \mathrm{GeV}\|$ [GeV]	–	–	–	–	–	> 7.5
$\mathrm{ANN}^{VH}_{\mathrm{DFOS}}$	> 0.2	–	–	–	–	–
$\mathrm{ANN}^{t\bar{t}}_{\mathrm{Zdep}}$	–	–	–	< 0.25	–	–

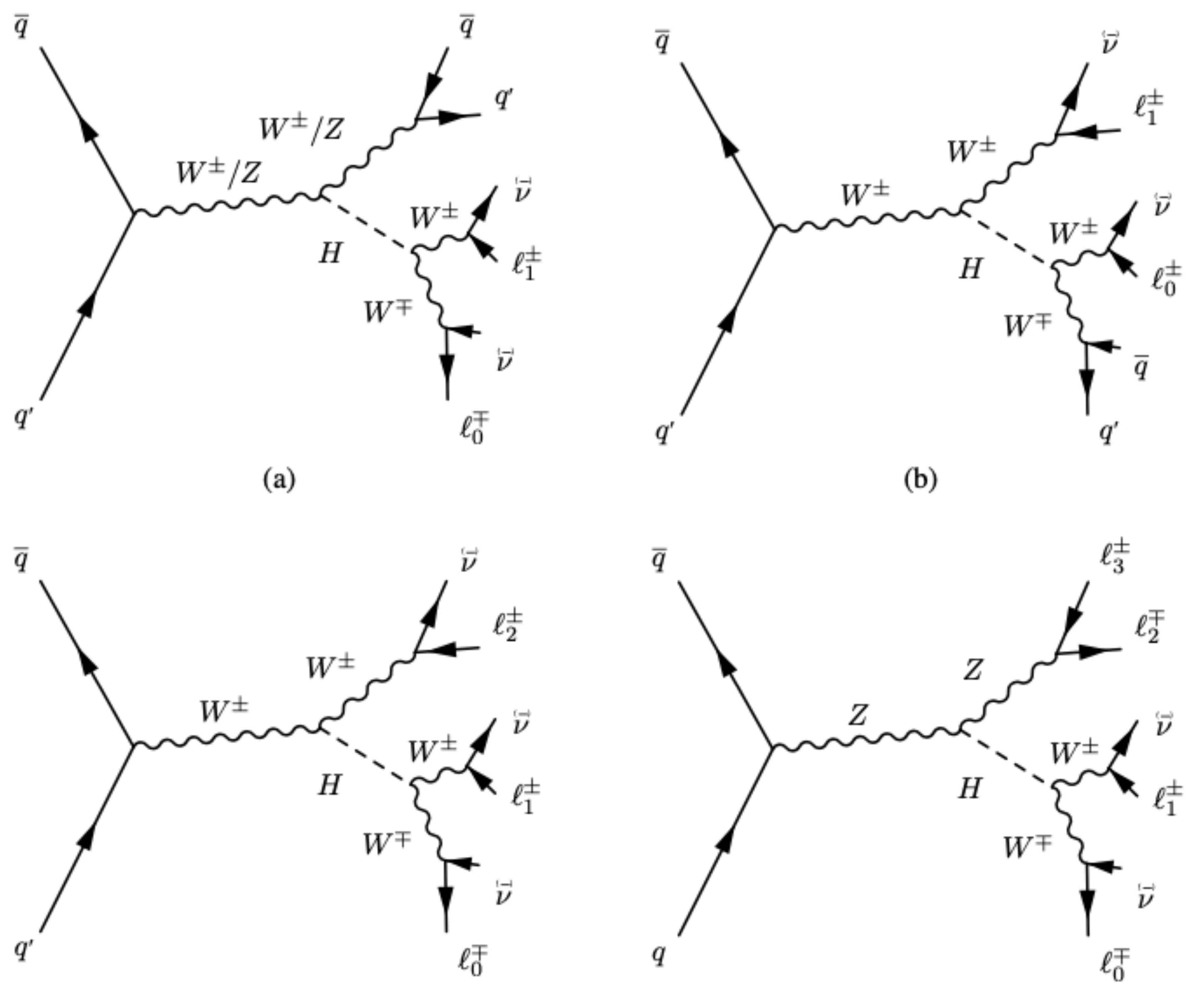

Figure 1: Leading-order Feynman diagrams for the signal topologies considered by the VH, $H \to WW^*$ measurement. The subscripts on the leptons are defined for the individual channels in Section 6: (a) the opposite-sign 2ℓ channel, (b) the same-sign 2ℓ channel, (c) the 3ℓ channel, and (d) the 4ℓ channel.

Channel	SR	SR discriminant	Relevant CR(s)
Opposite-sign 2ℓ	–	$\mathrm{ANN}_{\mathrm{DFOS}}$ (2(a))	Top, Z+jets, WW
Same-sign 2ℓ	SS2μ	RNN output (3(a))	–
	SS2e	RNN output (3(b))	
	SSDF	RNN output (3(c))	
3ℓ	Z-dominated	$\mathrm{ANN}_{\mathrm{Zdom}}$ (4(a))	WZ 0-jet, WZ ≥1-jets
	Z-depleted	$\mathrm{ANN}^{\Delta}_{\mathrm{Zdep}}$ (4(b))	
4ℓ	1-SFOS	1-SFOS BDT output (5(a))	ZZ
	2-SFOS	2-SFOS BDT output (5(b))	

VH $H \to WW$ measurement at 13 TeV

Channel	p_T^V proxy	Reconstructed SR	Relevant p_T^V range
Opposite-sign 2ℓ	Dijet transverse momentum, p_T^{jj}	$0 \leq p_T^{jj} < 160$ GeV	$0 \leq p_T^V < 150$ GeV
		$160 \leq p_T^{jj} < 260$ GeV	$150 \leq p_T^V < 250$ GeV
		$p_T^{jj} \geq 260$ GeV	$p_T^V \geq 250$ GeV
Same-sign 2ℓ	Scalar sum of lepton, jet, and missing transverse momenta, $\sum \lvert p_T \rvert$	$0 \leq \sum \lvert p_T \rvert < 200$ GeV	$0 \leq p_T^V < 75$ GeV
		$200 \leq \sum \lvert p_T \rvert < 320$ GeV	$75 \leq p_T^V < 150$ GeV
		$320 \leq \sum \lvert p_T \rvert < 460$ GeV	$150 \leq p_T^V < 250$ GeV
		$\sum \lvert p_T \rvert \geq 460$ GeV	$p_T^V \geq 250$ GeV
3ℓ Z-dominated	Regression ANN for W transverse momentum, p_T^R	$0 \leq p_T^R < 90$ GeV	$0 \leq p_T^V < 75$ GeV
		$90 \leq p_T^R < 180$ GeV	$75 \leq p_T^V < 150$ GeV
		$p_T^R \geq 180$ GeV	$p_T^V \geq 150$ GeV
3ℓ Z-depleted	Regression ANN for W transverse momentum, p_T^R	$0 \leq p_T^R < 90$ GeV	$0 \leq p_T^V < 75$ GeV
		$90 \leq p_T^R < 180$ GeV	$75 \leq p_T^V < 150$ GeV
		$180 \leq p_T^R < 270$ GeV	$150 \leq p_T^V < 250$ GeV
		$p_T^R \geq 270$ GeV	$p_T^V \geq 250$ GeV
4ℓ	Z boson transverse momentum, p_T^Z	$0 \leq p_T^Z < 75$ GeV	$0 \leq p_T^V < 75$ GeV
		$75 \leq p_T^Z < 150$ GeV	$75 \leq p_T^V < 150$ GeV
		$150 \leq p_T^Z < 250$ GeV	$150 \leq p_T^V < 250$ GeV
		$p_T^Z \geq 250$ GeV	$p_T^V \geq 250$ GeV

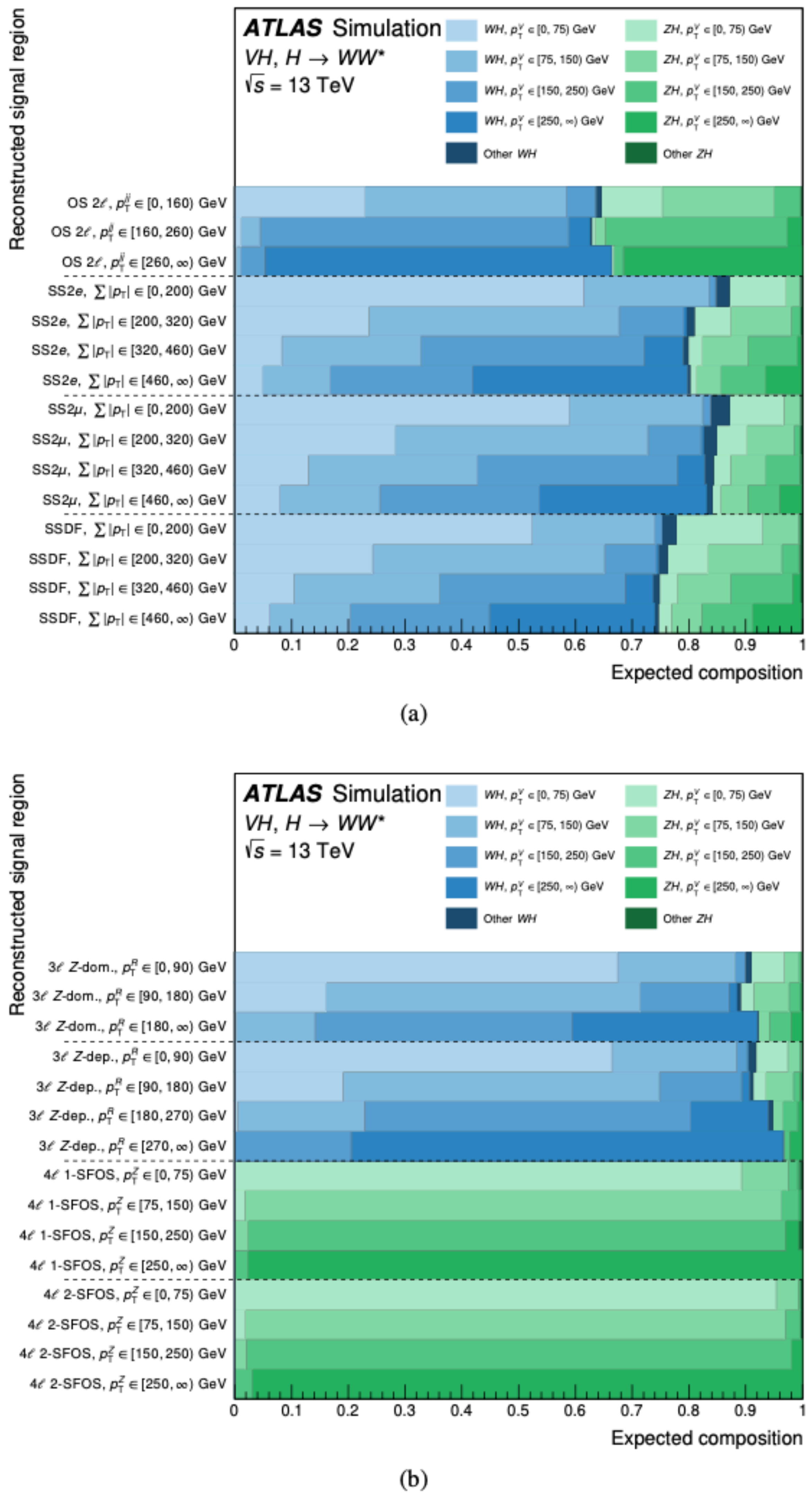

(a)
(b)

VH $H \to WW$ measurement at 13 TeV

Source	$\frac{\Delta(\sigma_{VH}\times\mathcal{B}_{H\to WW^*})}{\sigma_{VH}\times\mathcal{B}_{H\to WW^*}}$ [%]	$\frac{\Delta(\sigma_{WH}\times\mathcal{B}_{H\to WW^*})}{\sigma_{WH}\times\mathcal{B}_{H\to WW^*}}$ [%]	$\frac{\Delta(\sigma_{ZH}\times\mathcal{B}_{H\to WW^*})}{\sigma_{ZH}\times\mathcal{B}_{H\to WW^*}}$ [%]
Statistical uncertainties in data	22	54	29
Statistical uncertainties in SR data	20	46	28
Statistical uncertainties in CR data	10	29	6.3
Systematic uncertainties	13	35	10
Statistical uncertainties in simulation	6.2	13	5.9
Experimental systematic uncertainties	5.4	12	5.7
Electrons	1.1	1.6	1.6
Muons	2.7	3.0	4.1
Jet energy scale	1.0	3.1	0.5
Jet energy resolution	0.5	2.4	0.6
Flavour tagging	1.0	1.5	0.8
Missing transverse momentum	0.6	0.2	0.9
Pile-up	1.0	1.3	0.8
Luminosity	1.1	1.2	1.1
Mis-identified leptons	3.7	10	2.8
Charge-flip electrons	1.7	5.0	0.0
Theoretical uncertainties	6.9	20	4.2
WH	2.1	2.3	0.1
ZH	0.5	0.3	2.4
Other H	1.2	2.4	0.9
WW	1.2	3.7	0.2
WZ 0-jet	3.2	11	0.2
WZ $\geq$1-jets	3.2	9.7	0.4
ZZ	1.2	2.1	0.8
VVV	2.7	12	1.0
Top	2.8	5.0	2.4
Z+jets	1.6	2.9	1.5
RNN shape uncertainty for WZ	7.5	23	0.7
Total	26	64	30

A new Higgs Boson combination analysis

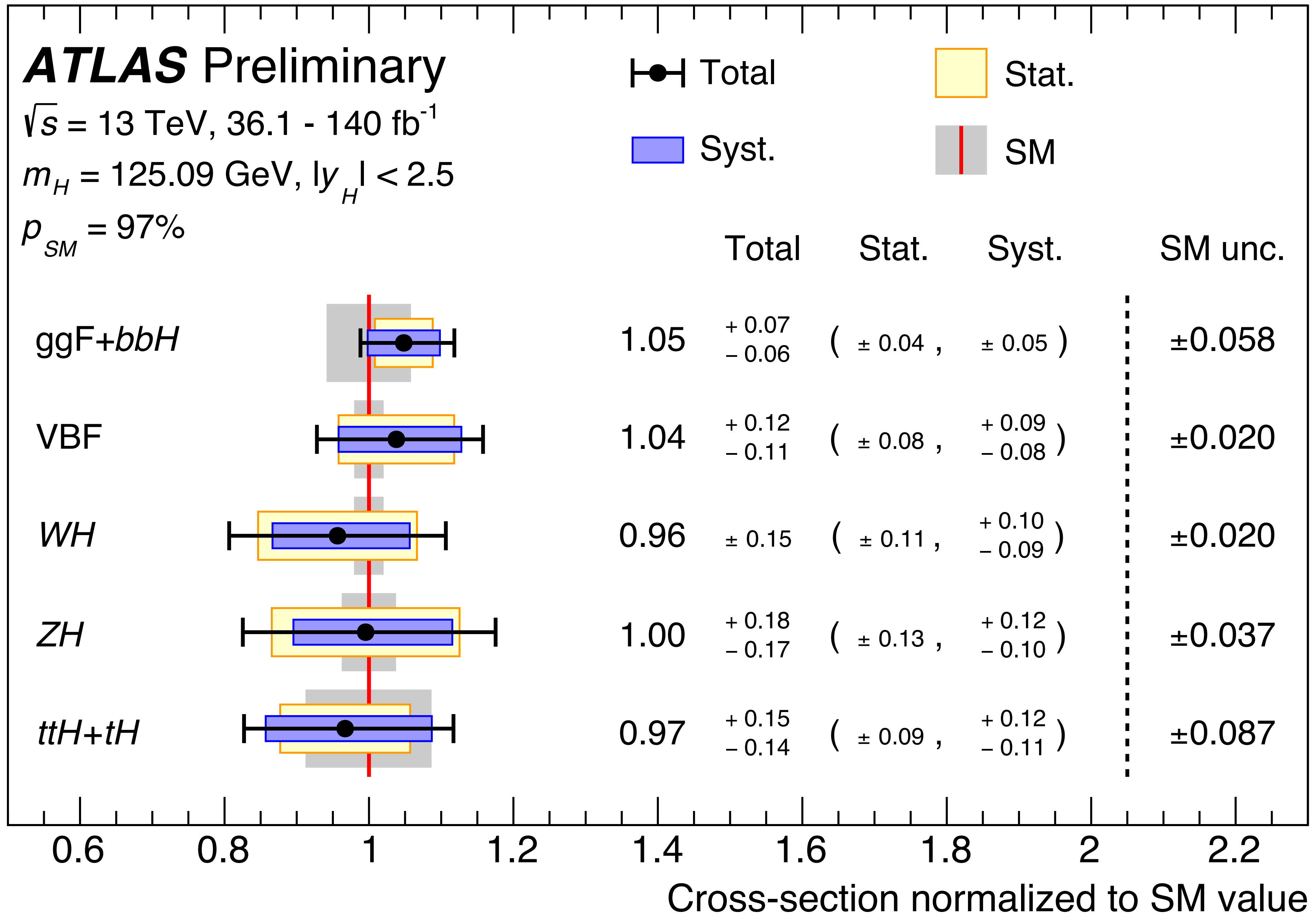

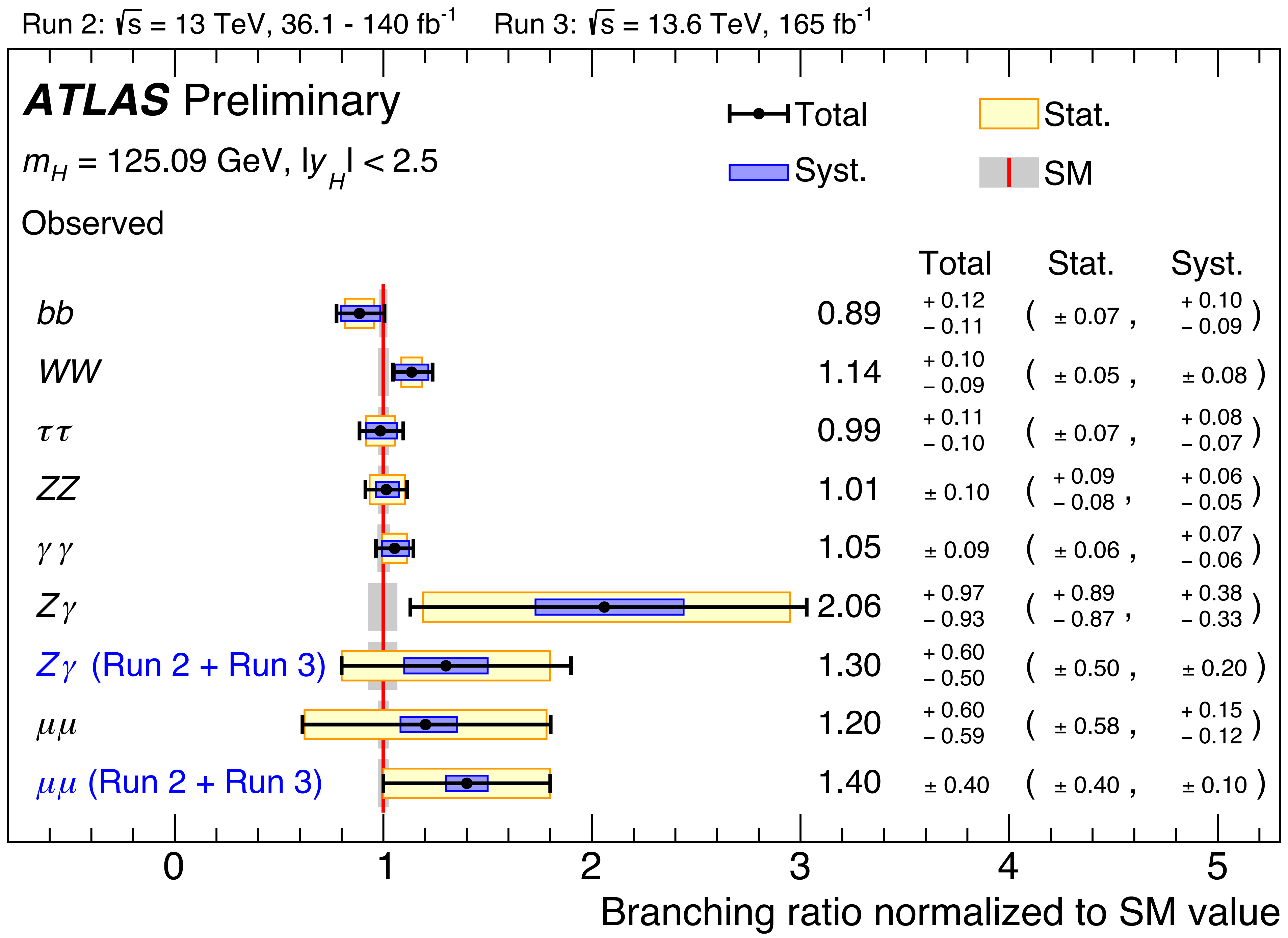

$$\mu = 1.023^{+0.056}_{-0.053} = 1.023 \pm 0.028\,(\text{stat.})\ ^{+0.026}_{-0.025}\,(\text{exp.})\ ^{+0.039}_{-0.036}\,(\text{sig. theo.})\ \pm 0.012\,(\text{bkg. theo.})$$

A new Higgs Boson combination analysis

Parameter	Resolved $\kappa_g, \kappa_\gamma, \kappa_{Z\gamma}$		Effective $\kappa_g, \kappa_\gamma, \kappa_{Z\gamma}$
	Free κ_c	$\kappa_c = \kappa_t$	$\kappa_c = \kappa_t$
κ_Z	$0.97^{+0.09}_{-0.07}$	0.96 ± 0.05	0.96 ± 0.05
κ_W	$0.99^{+0.09}_{-0.06}$	0.99 ± 0.04	1.00 ± 0.05
κ_t	$0.99^{+0.10}_{-0.08}$	$0.99^{+0.06}_{-0.05}$	0.99 ± 0.09
κ_b	$0.90^{+0.12}_{-0.11}$	0.89 ± 0.09	$0.89^{+0.10}_{-0.09}$
κ_c	$1.1^{+1.6}_{-3.8}$	—	—
κ_τ	$0.95^{+0.10}_{-0.08}$	0.94 ± 0.06	0.94 ± 0.06
κ_μ	$1.05^{+0.25}_{-0.31}$	$1.04^{+0.24}_{-0.30}$	$1.04^{+0.23}_{-0.30}$
κ_g	—	—	$0.99^{+0.07}_{-0.06}$
κ_γ	—	—	0.97 ± 0.06
κ_{Z/γ^*}	—	—	$1.36^{+0.30}_{-0.36}$